

I.

GAMMA RAY SPECTRA AND SHIELDING SURVEY
OF THE UNIVERSITY OF MARYLAND REACTOR

by

Nguyen Nhiep

Thesis submitted to the Faculty of the Graduate School
of the University of Maryland in partial fulfillment
of the requirements for the degree of
Master of Sciences
1963

APPROVAL SHEET

Title of Thesis: Gamma Ray Spectra and Shielding Survey
of the University of Maryland Reactor

Name of Candidate: Nguyen Nhiep
Master of Science, 1963

Thesis and Abstract Approved:

Dick Duffey
Dr. Dick Duffey
Professor of Nuclear
Engineering

Date Approved:

9 May 1963

ABSTRACT

Title of Thesis: Gamma Ray Spectra and Shielding Survey
of the University of Maryland Reactor

Nguyen Nhiep, Master of Science, 1963

Thesis directed by: Dr. Dick Duffey

The gamma ray spectra of the University of Maryland reactor were measured at the beam tube which extends from the side of the reactor to the core, the thermal column and the top of the reactor. There were three gamma ray spectra measurements at the beam tube: gamma ray spectra recorded by a single-channel spectrometer when the reactor was shut down and when the reactor was operated at different power levels and the gamma ray spectra recorded by a 256-channel spectrometer when the reactor was at different levels of power. However, only the single channel spectrometer was used to measure gamma ray spectra at the thermal column and the top of the reactor; some gamma ray spectra were recorded at the thermal column when the reactor was operated at various power levels and a gamma ray spectrum was recorded at the top of the reactor when the reactor was operated at full licensed power of 10 kw.

The gamma ray shielding survey of the reactor was done by a Geiger-Müller survey meter when the reactor was running at full power of 10 kw. The highest level found

was about 0.8 millirem per hour which was at the side of the reactor at core level. A calculated gamma ray level was near this value.

ACKNOWLEDGMENT

The author is indebted to Professor Dick Duffey for his suggestion of this topic and for his guidance in the preparation of this thesis.

TABLE OF CONTENTS

Chapter	Page
I. INTRODUCTION	1
1-1 Gamma Ray Sources	1
a. Prompt Fission Gamma Rays	1
b. Fission Product Decay Gamma Rays	1
c. Neutron Capture Gamma Rays	6
d. Inelastic Scattering Gamma Rays	7
e. Gamma Rays from Activated Materials	7
f. X-Rays	9
1-2 Interaction of Gamma Rays with Matter	9
a. Photoelectric Effect	10
b. Compton Scattering	11
c. Pair Production Process	13
d. Mass Attenuation Coefficients	14
II. EQUIPMENT	17
2-1 University of Maryland Reactor	17
Core	17
Thermal Column and Beam Tube	19
Shielding	21
2-2 Spectrometers	23
a. Detector	23
b. Analyzer	23
Single-Channel Pulse Height Ana- lyzer	23

TABLE OF CONTENTS CONTINUED

Chapter	Page
Multi-Channel Pulse Height	
Analyzer	26
2-3 G.M. Survey Meter	27
2-4 Calibration Sources	27
III. PROCEDURE AND EXPERIMENTAL DATA	28
3-1 Procedure	28
3-2 Single-Channel Spectrometer Gamma Ray	
Spectra	29
a. At the Beam Tube	29
b. At the Thermal Column	31
c. At the Top of the Reactor	31
3-3 Multi-Channel Spectrometer Gamma Ray	
Spectra	31
3-4 Shielding Survey	37
IV. DISCUSSION	48
4-1 Gamma Ray Spectra	48
4-2 Shielding Survey	50
V. CONCLUSIONS AND RECOMMENDATIONS	51
APPENDIX	53
SELECTED BIBLIOGRAPHY	56

LIST OF TABLES

Table	Page
1-1 Energy Spectrum of Prompt Gamma Rays from Fission of U^{235}	2
1-2 Energy Groups	4
1-3 Compton Effect	5
1-4 Energy Change in Inelastic Scattering Process	8
1-5 Photoelectric Effect	8
1-6 Compton Scattering	10
1-7 Pair Production Process	12
1-8 Mass Absorption Coefficients for H_2O	16
2-1 Reactor Core Cross Section from the Top	18
2-2 Vertical Cross Section of the Thermal Column	20
2-3 Horizontal Cross Section of the Beam Tube	20
2-4 Plan of the University of Maryland Reactor	22
2-5 Schematic Diagram of a Scintillation Detector and Schematic Diagram of a Photomultiplier	24
2-6 Schematic Diagram of a Single-Channel Analyzer	25
2-7 Schematic Diagram of a Multi-Channel Analyzer	25
3-1 Gamma Spectrum I	30
3-2 Gamma Spectrum II	32
3-3 Gamma Spectrum III	33
3-4 Gamma Spectrum IV	34
3-5 Gamma Spectrum V	35
3-6 Gamma Spectrum VI	36
3-7 Gamma Spectrum VII	38
3-8 Gamma Spectrum VIII	39

LIST OF FIGURES

Figure	Page
1-1 Energy Distribution of Prompt Gamma Rays from Fission of U-235	3
1-2 Decay of Fission Product Gamma Rays after Infinite Irradiation Time	5
1-3 Energy Change in Inelastic Scattering Process . .	8
1-4 Photoelectric Effect	8
1-5 Compton Scattering	12
1-6 Pair Production Process	12
1-7 Mass Attenuation Coefficients for NaI	16
2-1 Reactor Core Seen from the Top	18
2-2 Vertical Cross Section of the Thermal Column . .	20
2-3 Horizontal Cross Section of the Beam Tube	20
2-4 Plan of the University of Maryland Reactor . . .	22
2-5 Schematic Diagram of a Scintillation Detector and Schematic Diagram of a Photomultiplier . . .	24
2-6 Schematic Diagram of a Single-Channel Analyzer .	25
2-7 Schematic Diagram of a Multi-Channel Analyzer . .	25
3-1 Gamma Spectrum I	30
3-2 Gamma Spectrum II	32
3-3 Gamma Spectrum III	33
3-4 Gamma Spectrum IV	34
3-5 Gamma Spectrum V	35
3-6 Gamma Spectrum VI	36
3-7 Gamma Spectrum VII	38
3-8 Gamma Spectrum VIII	39

LIST OF FIGURES CONTINUED

Figure	Page
3- 9 Gamma Level I - Face I	40
3-10 Gamma Level I - Face II	40
3-11 Gamma Level I - Face III	41
3-12 Gamma Level I - Face IV	42
3-13 Gamma Level I - Face V	43
3-14 Gamma Level I - Face VI	44
3-15 Gamma Level II	45
3-16 Gamma Level III	45
3-17 Gamma Level at the Concrete Top of the Reactor .	46

of the order of one microsecond after the fission, gamma rays are given off from the fissioning nucleus. These gamma photons are called prompt. For ^{235}U , the energy distribution of prompt photons from thermal neutron induced fission is shown in Table 1. From the data, the total gamma ray energy per fission is about 7.46 Mev. On the average, 7.51 photons are emitted per fission with energies between 0.2 and 7.6 Mev and the approximate form of this distribution (Fig. 1-1) in the range of fission gamma ray energy is

$$Y(E) = 0.9e^{-1.06E}$$

where $Y(E)$ is number of photons escaping per 0.1 Mev energy interval at energy E , the photon energy in Mev.

b. Fission product decay gamma rays. The fission of a heavy element can take place to form a large variety of

I INTRODUCTION

Of the nuclear fission reactor radiations of engineering interest, gamma rays and neutrons are more penetrating than alpha and beta particles and protons resulting from neutron proton (n,p) reactions. Therefore, consideration of the gamma ray intensity and spectra of a reactor is necessary in the shielding design. Gamma rays emitted from the nuclear reactor core are from several sources and their energies vary.

1-1 Gamma Ray sources follow:

a. Prompt fission gamma rays [1]. Within a time of the order of one microsecond after the fission, gamma rays are given off from the fissioning nucleus. These gamma photons are called prompt. For U^{235} , the energy distribution of prompt photons from thermal neutron induced fission is shown in Table 1. From the data, the total gamma ray energy per fission is about 7.46 Mev. On the average, 7.51 photons are emitted per fission with energies between 0.2 and 7.6 Mev and the approximate form of this distribution (Fig. 1-1) in the range of fission gamma ray energy is

$$Y(E) = 0.9e^{-1.08E}$$

where $Y(E)$ is number of photons escaping per 0.1 Mev energy interval at energy E , the photon energy in Mev.

b. Fission product decay gamma rays. The fission of a heavy element can take place to form a large variety of

TABLE 1-1

Energy Spectrum of Prompt Gamma Rays From Fission of U^{235}

Gamma Ray Energy Mev	Gamma Rays per 0.1 Mev	Gamma Ray Energy Mev	Gamma Rays per 0.1 Mev	Gamma Ray Energy Mev	Gamma Rays per 0.1 Mev
0.2	0.815	2.7	0.0409	5.2	0.00430
0.3	0.697	2.8	0.0369	5.3	0.00399
0.4	0.661	2.9	0.0330	5.4	0.00371
0.5	0.622	3.0	0.0298	5.5	0.00341
0.6	0.553	3.1	0.0268	5.6	0.00314
0.7	0.474	3.2	0.0244	5.7	0.00290
0.8	0.408	3.3	0.0219	5.8	0.00264
0.9	0.353	3.4	0.0198	5.9	0.00243
1.0	0.307	3.5	0.0181	6.0	0.00223
1.1	0.272	3.6	0.0165	6.1	0.00204
1.2	0.240	3.7	0.0150	6.2	0.00188
1.3	0.205	3.8	0.0136	6.3	0.00172
1.4	0.180	3.9	0.0126	6.4	0.00157
1.5	0.158	4.0	0.0116	6.5	0.00139
1.6	0.139	4.1	0.0106	6.6	0.00128
1.7	0.125	4.2	0.00985	6.7	0.00115
1.8	0.113	4.3	0.00908	6.8	0.00103
1.9	0.102	4.4	0.00830	6.9	0.000916
2.0	0.0907	4.5	0.00760	7.0	0.000833
2.1	0.0818	4.6	0.00704	7.1	0.000731
2.2	0.0726	4.7	0.00649	7.2	0.000629
2.3	0.0651	4.8	0.00604	7.3	0.000547
2.4	0.0579	4.9	0.00556	7.4	0.000467
2.5	0.0512	5.0	0.00519	7.5	0.000338
2.6	0.0457	5.1	0.00470	7.6	0.000308
				Total	7.336 Mev

Energy Distribution of Prompt Gamma Rays
from Fission of U-235
(from Table 1-1)

Photons escaping per 0.1 Mev energy interval at energy E

1/10

1/10²

1/10³

1/10⁴

approximate

experimental

Energy in Mev

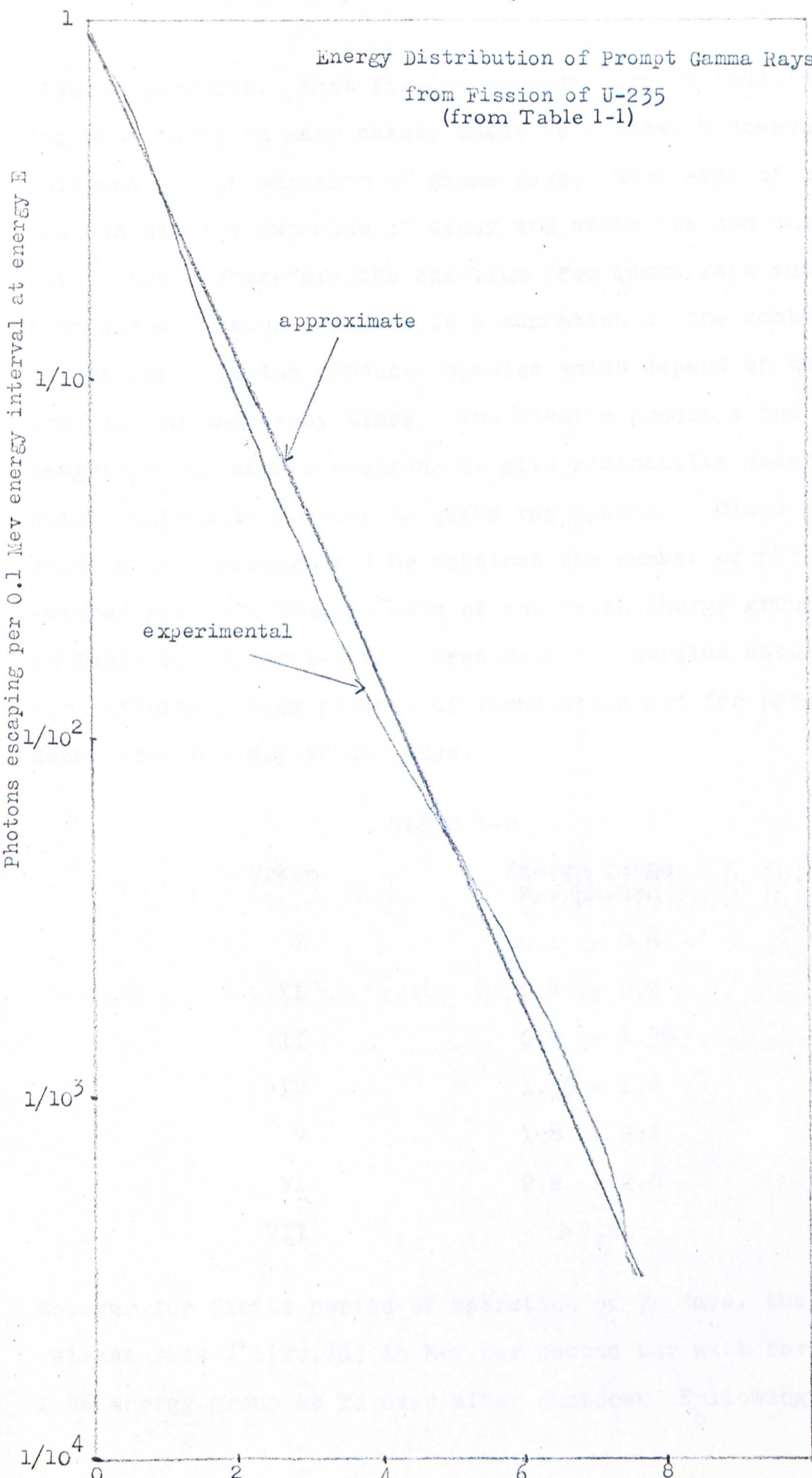
0

2

4

6

8



fission products. Most fission products are radioactive emitting beta rays; in many cases, these beta decay processes are followed by the emission of gamma rays. Each type of unstable nucleus has its own mode of decay and emits its own characteristic rays. Therefore, the spectrum from gamma rays emitted from mixed fission products is a summation of the contribution of the many fission product species which depend on the irradiation and decay times. The fission products and their daughters may absorb neutrons to give radioactive materials which contribute further to gamma ray spectra. Clark [1,2] studied this problem and he obtained the number of photons emitted per unit time in each of the seven energy groups shown in Table 2; Figure 1-2 is a breakdown of energies assumed, for infinitely long periods of irradiation and for periods of decay from 0.1 day to 100 days.

TABLE 1-2

Group	Energy range Mev/photon
I	0.1 - 0.4
II	0.4 - 0.9
III	0.9 - 1.35
IV	1.35 - 1.8
V	1.8 - 2.2
VI	2.2 - 2.6
VII	>2.6

However for finite period of operation of T_0 days, the energy release rate $\Gamma_i(T_0, T_d)$ in Mev per second per watt for the i th energy group at T_d days after shutdown, following T_0 days

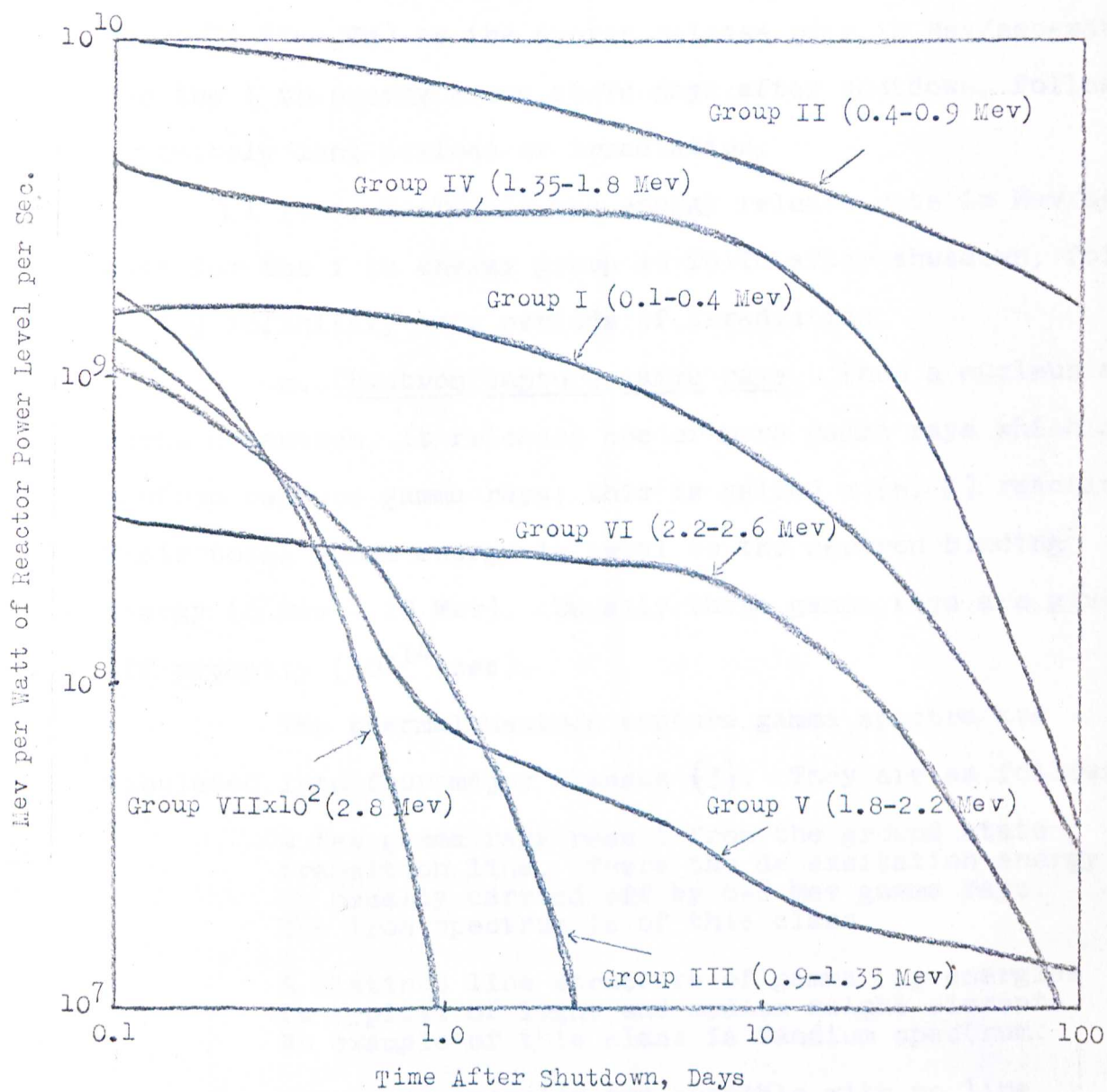


Fig. 1.2 [2]

Decay of Fission Product Gamma Rays after Infinite
Irradiation Time

of steady rate operation is given by the following relation:

$$\Gamma_i (T_0, T_d) = \Gamma_i (\infty, T_d) - \Gamma_i (\infty, T_0 + T_d) \quad (2)$$

where $\Gamma_i (\infty, T_d)$ is the energy release rate in Mev/sec-watt for the i th energy group at T_d days after shutdown, following infinitely long periods of irradiation,

$\Gamma_i (\infty, T_0 + T_d)$ is the energy release rate in Mev/sec-watt for the i th energy group at $T_0 + T_d$ after shutdown, following infinitely long periods of irradiation.

c. Neutron capture gamma rays. When a nucleus absorbs a neutron, it releases one or more gamma rays which are neutron capture gamma rays; this is called a (n, γ) reaction. Their total gamma energy is equal to the neutron binding energy (6 Mev - 10 Mev). Usually these gamma rays are given off promptly (10^{-14} sec).

The thermal neutron capture gamma spectra are tabulated into four major classes (3). They are as follows:

A few gamma rays result from the ground state transition line. There the de-excitation energy is usually carried off by 6-8 Mev gamma rays. The iron spectrum is of this class.

A distinct line structure of gamma ray energies is typical of light and medium weight elements. An example of this class is Vanadium spectrum.

Gamma ray energies are possible with no line structure evident below 5 Mev which is typical of heavier elements, e.g. Cadmium.

The gamma rays may be weak or non-existent because particle emission is the favored mode of de-excitation, e.g. neutron alpha (n, α) or neutron proton (n, p) reactions. Neutron absorptions by Boron 10 and Lithium 6 are representatives of this class.

The concentration of gamma ray emitting nuclides from capture is given by

$$S = \sum_i N_i \sigma_i \phi \quad (3)$$

where S = the resulting nuclei/cm³ - sec;

N_i = the number of nuclei per cubic centimeter of i th element in which the thermal neutron capture is taking place;

σ_i = the microscopic cross section of i th element in barns per nucleus of a (n, γ) reaction;

ϕ = local neutron flux in neutron/cm²-sec; the flux is primarily thermal in the University of Maryland reactor.

d. Inelastic scattering gamma rays Fast neutrons may lose kinetic energy by inelastic scattering, leaving the struck nucleus in an excited state (Fig. 1-3). In other words, in an inelastic scattering process, part of the kinetic energy of the neutron is converted into excitation energy of the struck nucleus. This excitation energy is subsequently emitted as one or more photons of gamma radiation, called inelastic scattering gamma rays. It is important to note that the initial energy of the neutron must exceed the minimum excitation energy of the struck nucleus. For elements of moderate and high mass number only neutrons which possess at least about 0.1 Mev of energy, can be inelastically scattered. With decreasing mass number of the nucleus, the required neutron energy is increased. Therefore, the total gamma ray energy emitted by an element of low mass number is higher than that emitted by a heavy element in an inelastic scattering process.

e. Gamma rays from activated materials. Many elements in the reactor structure become radioactive when they absorb neutrons, and decay with the release of beta and gamma rays or both. The structure is primarily aluminum, and its

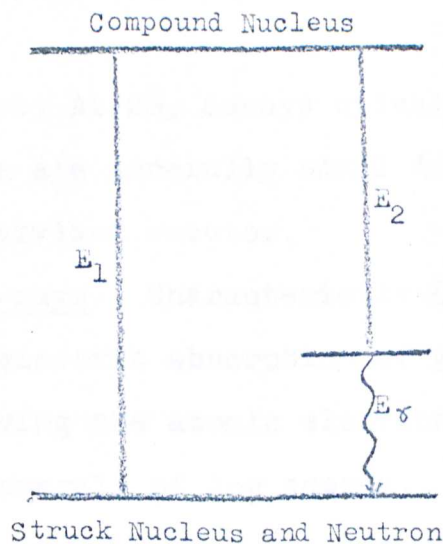


Fig. 1.3 (4)

Energy Change in Inelastic Scattering Process

E_1 : the total kinetic energy of the struck nucleus and neutron

E_2 : the kinetic energy of the compound nucleus

E_γ : the energy emitted as gamma radiation

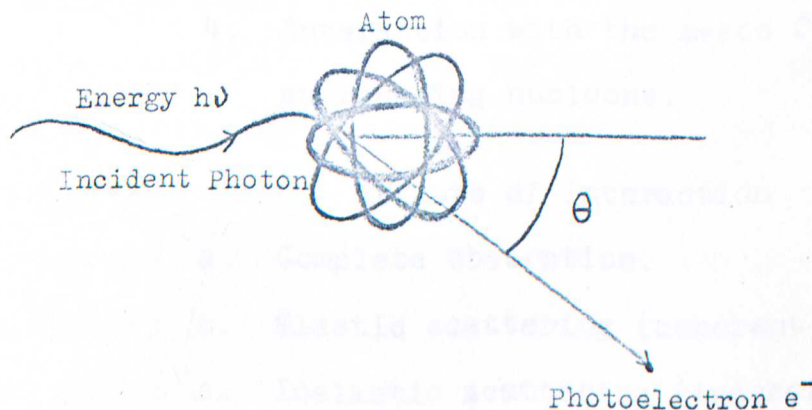


Fig. 1.4

Photoelectric Effect

activated product, Al-28, decays quickly. Thus, these induced activities are generally small in the core of the University of Maryland reactor.

f. X-rays. Characteristic X-rays are produced following photoelectric absorption of gamma rays or other processes involving the atomic electrons. However, these X-rays are in general, of low energy.

1-2 Interaction of gamma rays with matter

The possible processes of gamma ray interaction with matter as described by Fano [5]:

Kinds of gamma ray interaction

1. Interaction with atomic electrons.
2. Interaction with nucleons.
3. Interaction with the electric field surrounding nuclei or electrons.
4. Interaction with the meson field surrounding nucleons.

Effects of Interaction

- a. Complete absorption.
- b. Elastic scattering (coherent).
- c. Inelastic scattering (incoherent).

Then there are a variety of different processes of absorption and scattering of gamma rays from this combination. However, in the energy domain of 0.05 Mev to 4 Mev, usually met with nuclear reactor, three processes give a fairly satisfactory description of the absorption and scattering of gamma rays in matter. These are Compton Effect (1,c), the Photoelectric

Effect (1,a) and Pair Production Effect (3,a). The numbers and letters refer to the above table.

a. Photoelectric Effect. The photoelectric effect predominates below energies of about 0.1 Mev in medium and high atomic number (Z) materials. Photoelectric effect occurs when a gamma ray transfers all of its energy to an electron and disappears (Fig. 1-4). Photons cannot interact with free electrons, because another body must be present if momentum is to be conserved. Therefore the interaction between photons and electrons occurs with strongly bound electrons and the interaction probability will increase with the electron binding energy, and about 80% of photoelectric interaction takes place with the K-shell provided that the gamma ray energy exceeds the K-binding energy and a large part of the remaining 20% of interactions takes place with the L-shell. The excited atoms then emit characteristic X-rays and Auger electrons in the filling of the vacancy in the inner shell. The Auger electrons have relatively short ranges and usually they are absorbed easily, but the characteristic X-rays are more penetrating. For example if they originate near the walls of a detector they will have appreciably probability of escaping without an interaction. However each successive photon has a lower energy and the probability of escape becomes small very quickly.

The value of absorption coefficient μ_{ϕ} in cm^{-1} due to the photoelectric effect is a function of both atomic number Z and energy $h\nu$. For $E_b < h\nu < m_0c^2$ (where m_0c^2 is 0.51 Mev, the rest mass energy of an electron). The expression [6] for

the rate of interaction μ_ϕ is

$$\mu_\phi \sim NZ^5 (h\nu)^{-3.5} \quad (4)$$

where N is the number of atoms per unit volumes and E_b is the binding energy of the orbital electrons.

b. Compton Scattering. In the Compton effect, the photon of energy $h\nu$ incident upon a free or loosely bound electron, results in a new photon of lesser energy $h\nu'$ at an angle ϕ with the incident photon (Fig. 1-5). Compton scattering generally involves the outer electrons which are lightly bound and does not produce a significant amount of K or L shell X-rays, except in the light elements. The energy $h\nu'$ can be calculated from the conservation of momentum and energy equations

$$h\nu' = \frac{h\nu}{1 + \frac{h\nu}{m_0c^2} (1 - \cos \phi)} \quad (5)$$

The rest energy of the electron, m_0c^2 , is 0.51 Mev. The above equation has been derived on the assumption that the scattering electrons are free and initially at rest. In fact, electrons of matter are bound and they have energy and momentum. But when the Compton process is predominant, the energy of the incident photon is much greater than the electron binding energies. From equation (5), it is seen that a single Compton scattering absorbs only a portion of the incident photon energy. The fraction of energy absorbed in any particular interaction depends on the incident photon energy and the scattering angle. The average fraction of the incident photon energy lost per Compton interaction varies from 14 percent at 100 Kev to 68 percent at 10 Mev.

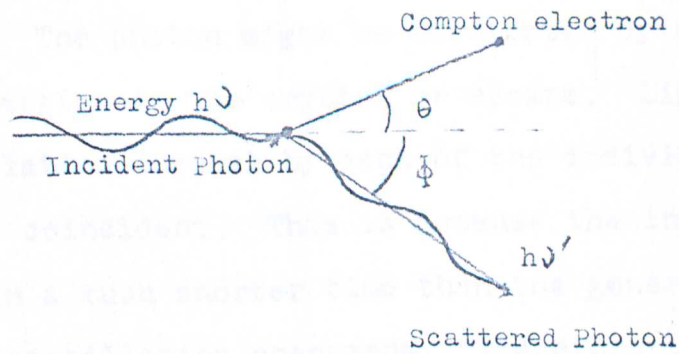


Fig. 1.5

Compton Scattering

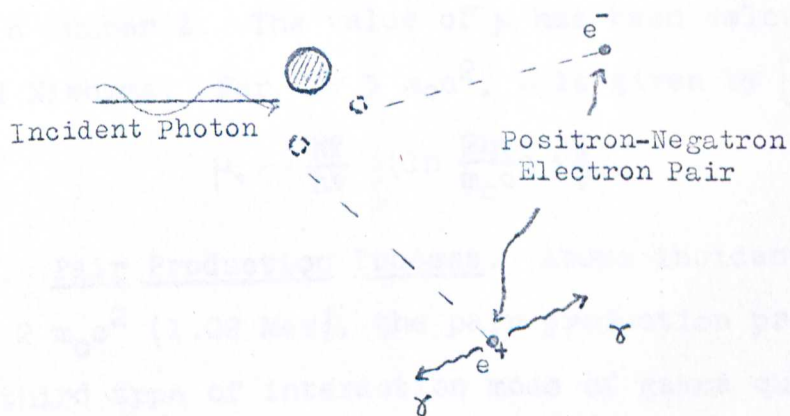


Fig. 1.6

Pair Production Process

If a single incident photon enters a scintillation crystal detector, the Compton interaction may be repeated several times. The photon might be terminated by either photoelectric interaction in the crystal or escape. Light generated in the scintillation crystal by each of the individual events is essentially coincident. This is because the interaction events occur in a much shorter time than the generation and decay of the scintillation phenomena. Therefore the scintillation effect is greater than expected from the photoelectric interaction alone, because an appreciable number of Compton interactions occur in the scintillation detector from one photon.

Since each electron enters individually into the scattering process, the absorption coefficient or rate of interaction μ_c due to the Compton scattering is proportional to the atomic number Z . The value of μ_c has been calculated by Klein and Nishima. For $h\nu > m_0c^2$, μ_c is given by [6]

$$\mu_c \sim \frac{NZ}{h\nu} \left(\ln \frac{2h\nu}{m_0c^2} + \frac{1}{2} \right) \quad (6)$$

c. Pair Production Process. Above incident photon energies of $2 m_0c^2$ (1.02 Mev), the pair production process which is a third type of interaction mode of gamma quanta with matter, becomes increasingly important. The energy $2 m_0c^2$ is a threshold for the process. In this interaction, the photon is completely absorbed and creates a positron (positive electron), negatron (negative electron) pair whose total energy is just equal to $h\nu$

$$h\nu = (T_- + m_0c^2) + (T_+ + m_0c^2) \quad (7)$$

where T_- is the kinetic energy of the negatron and

T_+ is the kinetic energy of the positron.

The negatron and positron lose their kinetic energies by collisions with other electrons and ultimately come to rest, at which time the positron interacts with a neighboring electron. There is annihilation of a positron and electron and two annihilation photons, each with an energy of 0.51 Mev are emitted in approximately opposite directions (Fig. 1-6).

Since there may be total absorption of both annihilation gamma rays or escape of one or escape of both of them. Usually two additional peaks $E-2m_0c^2$, $E-m_0c^2$ can be recognized in the gamma ray spectra curve at 0.51 Mev intervals; E is the energy of gamma ray being measured.

For $h\nu \leq 1.02$ Mev, the absorption coefficient μ_{π} due to the pair production process is zero. For the gamma rays of energy greater than 1.02 Mev, μ_{π} increases linearly at the low energies and rises as $\ln E$ at the higher energies. Thus the expression [6] for μ_{π} is

$$\mu_{\pi} \sim NZ^2(h\nu - 2m_0c^2) \quad (8)$$

in the vicinity of 1 Mev and

$$\mu_{\pi} \sim NZ^2 \ln h\nu \quad (9)$$

at very high energies.

d. Mass attenuation coefficients. The total mass attenuation coefficient $\frac{\mu}{\rho}$ (cm^2/gm) can be expressed as

$$\frac{\mu}{\rho} = \frac{1}{\rho} (\mu_{\phi} + \mu_c + \mu_{\pi}) \quad (10)$$

where ρ is the density of the absorber in gm/cm^3 .

The probability of transmission would then be

$$e^{-\frac{\mu}{\rho} x}$$

with x , the absorber thickness in gram square centimeter. Fig. 1-7 [7] is shown for sodium iodide (NaI), a typical scintillation material in which the individual mass attenuation coefficients $\frac{\mu_{\phi}}{\rho}$, $\frac{\mu_c}{\rho}$ and $\frac{\mu_{\pi}}{\rho}$ as well as the total coefficient are given.



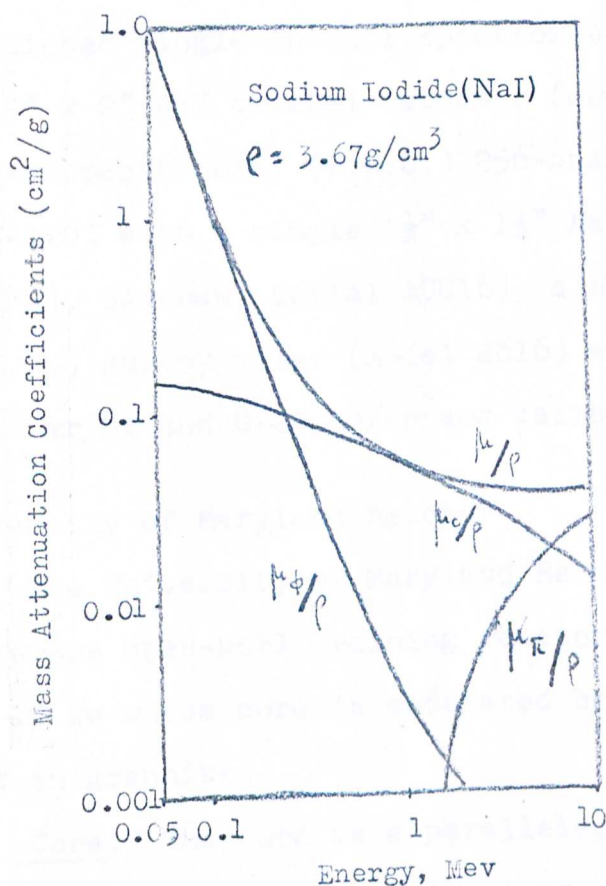


Fig. 1.7 [7]

Mass Attenuation Coefficients for NaI

- μ_0 = total absorption coefficient in cm^{-1}
- μ_a = absorption coefficient due to the photo-electric effect in cm^{-1}
- μ_c = absorption coefficient due to the Compton scattering in cm^{-1}
- μ_R = absorption coefficient due to the pair production process in cm^{-1}

II EQUIPMENT

This study was with the University of Maryland reactor (UMR) and the experimental equipment consisted of a Nuclear Chicago single-channel spectrometer (model 132) with a single 2" x 2" NaI crystal detector (model D55), a Technical Measurements Corp. (T.M.C.) 256-channel spectrometer (model CN-110) with a single 1½" x 1½" NaI crystal detector (Type 6D4F9), Harshaw, Serial AUG16), a Nuclear Chicago Geiger-Müller (G.M.) survey meter (model 2616) with a range of 0-0.2 mr/hr, 0-2 mr/hr and 0-20 mr/hr and calibration sources.

2-1 University of Maryland Reactor

The University of Maryland Reactor [8] UMR is a heterogeneous open-pool training reactor licensed for operation at 10 kw whose core is moderated by ordinary water and reflected in graphite.

Core. The core is a parallelepiped, 23-5/8 in. high, about 18 in. wide and 18 in. long, consisting of thirteen 10-plate fuel elements, one nine-plate element, one five-plate element, one four-plate fuel element, three fuel elements containing 6 fuel plates with spaces for control rods, and graphite reflection blocks. The core is reflected on each of three sides (west, north and east) by a single row of 23-5/8 in. high, 3 in. square graphite blocks (except for the space where the 4 plate element is), on the fourth side by the thermal column graphite (Fig. 2-1) and at the top and bottom

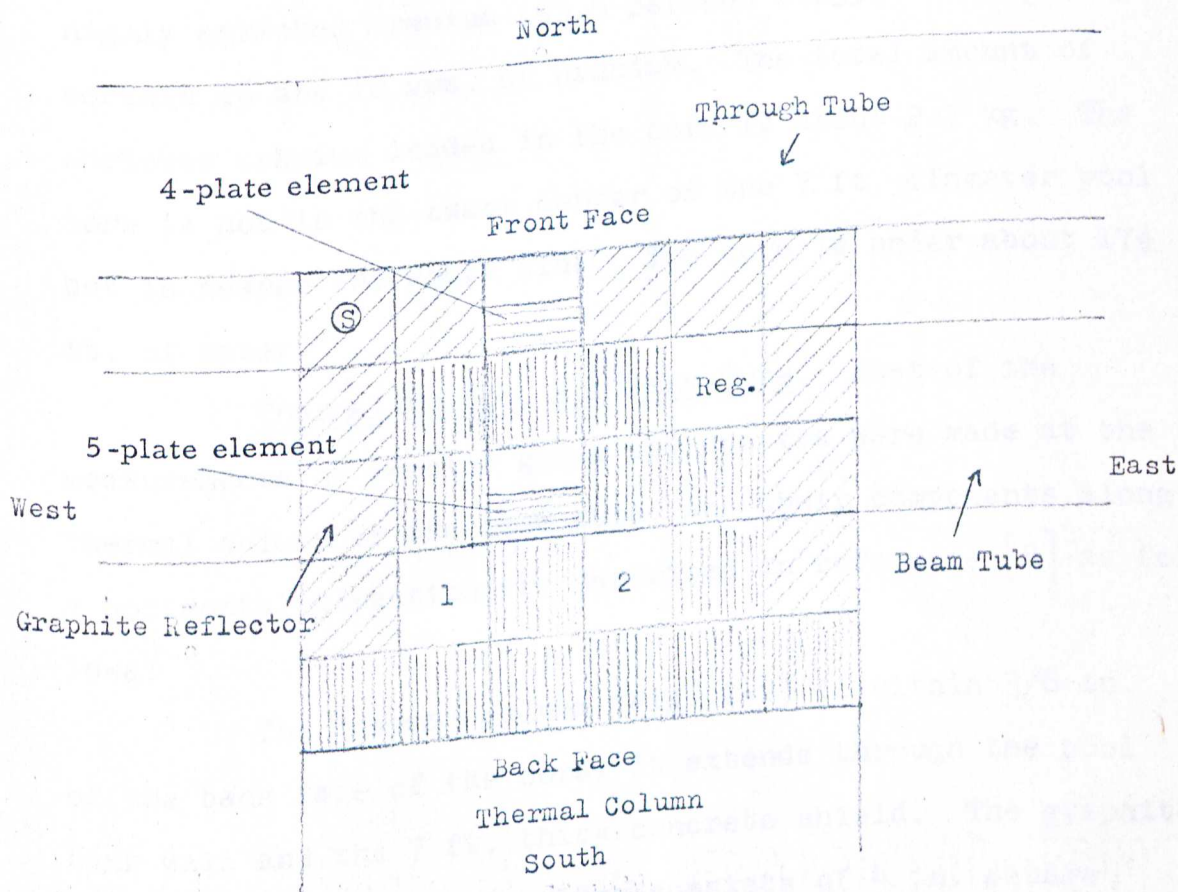


Fig. 2.1
Reactor Core Seen from the Top



Fuel



Graphite



1 and 2 are shim safety rod elements
Reg. refers to regulating rod elements.

by the pool water and the aluminum in the fuel elements and support components. The thermal column area of the core end is 24 in. x 24 in. The fuel in the plates is an alloy of highly enriched uranium (93.5 percent U-235). The plates contain 16 and 18 gms. of uranium. The total amount of enriched uranium loaded in the core is about 2.7 kg. The core is not in the exact center of the 7 ft. diameter pool but is nearer the south side. The core is under about $17\frac{1}{2}$ ft. of water.

Thermal Column and Beam Tube. Most of the measurements of reactor gamma ray spectra were made at the thermal column or the beam tube, and their components along a horizontal direction are described in reference [8] as follows:

The thermal column (Fig. 2-2) is within $\frac{3}{8}$ in. of the back face of the core; it extends through the pool tank wall and the 7 ft. thick concrete shield. The graphite assembly of the thermal column consists of 4 in. square stringers arranged in the form of a stepped column 60 in. long. The section forward of the step is $37\frac{3}{4}$ in. long and 24 in. square; in it the stringers are arranged in a 6 x 6 pattern. The outer section of the graphite column is $22\frac{1}{2}$ in. long and 32 in. square, and its stringers are arranged in an 8 x 8 pattern. There are small slots and holes in the stringers for measurements, e.g. with foils.

The thermal column shield plug at the outer end of the thermal column is 41 in. long and $39\frac{3}{4}$ in. square. It is concrete covered on the core side with $\frac{1}{8}$ in. of boral. The plug contains a smaller, carbon steel covered

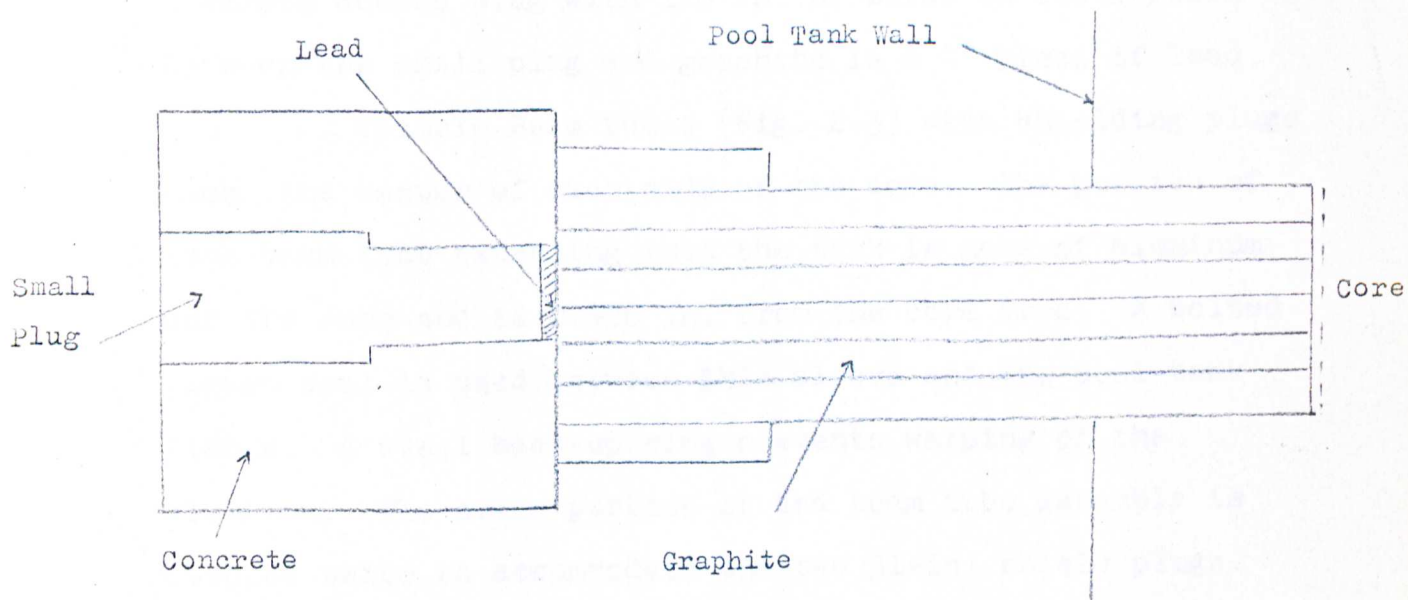


Fig. 2.2
Vertical Cross Section of the Thermal Column

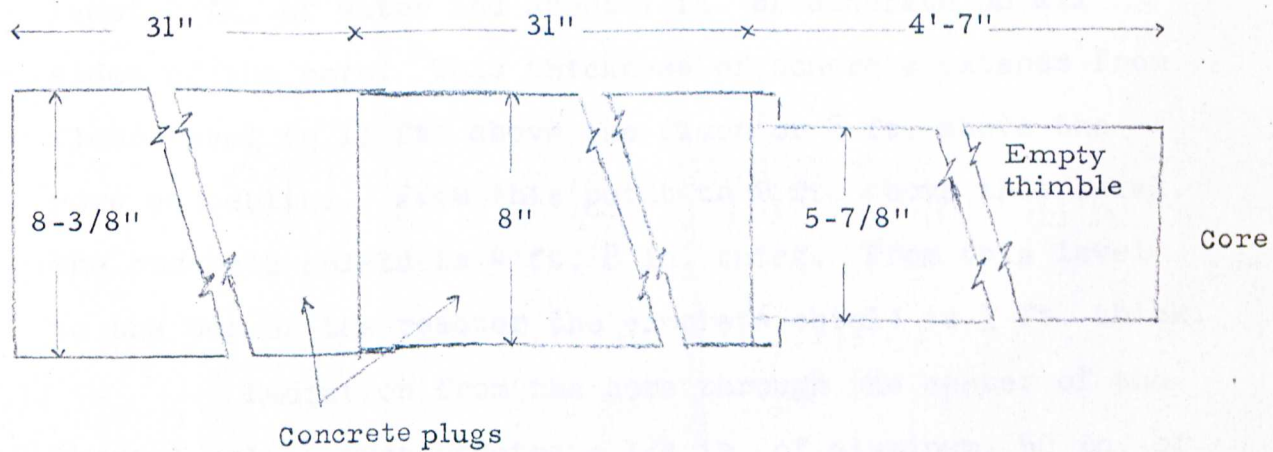


Fig. 2.3
Horizontal Cross Section of the Beam Tube

concrete access plug with $1/8$ in. of boral on its forward end. Between the small plug and graphite is a 4" piece of lead.

Thimble Beam tubes (Fig. 2-3) with shielding plugs face the center of each side of the core. The portion of each beam tube extending into the tank is made of aluminum and its core end is 0.426 in. from the core face. A bolted gasket seal is used between this sleeve and the pool-tank flange. A steel back-up ring prevents warping of the aluminum. The outer portion of the beam tube assembly is stepped twice to accommodate the two 31-in. shield plugs. These plugs are of aluminum clad concrete.

Shielding (Fig. 2-4). The shielding consists of ordinary concrete and water. The pool tank (7 ft. diameter and 21 ft. high) and the reactor structure provide at least 2 ft. of water and about 7 ft. of concrete on all sides of the core. This thickness of concrete extends from floor level to 11 ft. above the floor or 8 ft. above the core centerline. From this point to 2 ft. above this level, the concrete shield is 4 ft. 8 in. thick. From this level to the top of the reactor the concrete shield is 3 ft. thick.

Radiation from the core through the center of the thermal column must penetrate $1/4$ in. of aluminum, 50 in. of graphite, $1/8$ in. of boral, 1 in. of steel, 4 in. of lead and $38-5/8$ in. of concrete.

Radiation through the centerline of the beam tube from the core must penetrate $3/8$ in. of water, $1/4$ in. of aluminum, $1/8$ in. of boral, 58 in. of concrete, 4 in. of lead and 2 in. of steel.

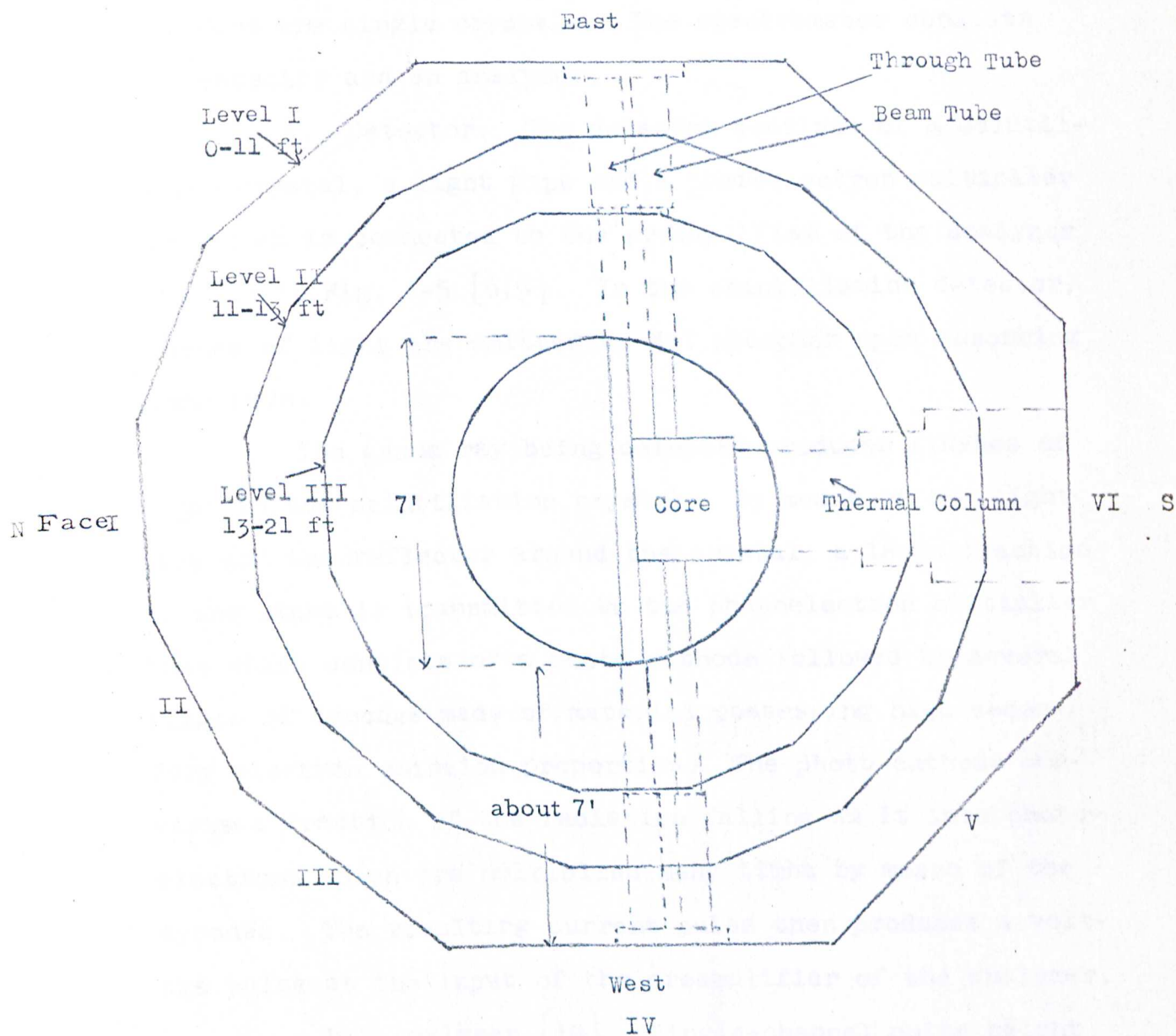


Fig. 2.4

Plan of the University of Maryland Reactor

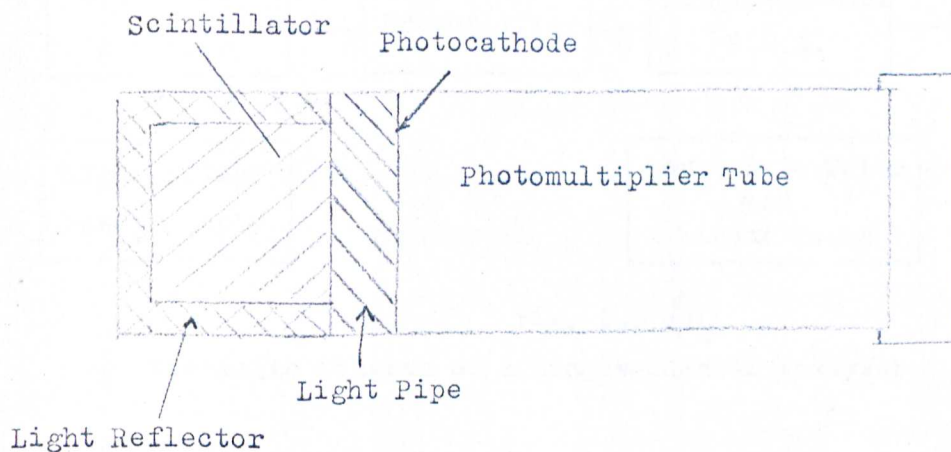
2-2 Spectrometers

Two spectrometers, a single channel spectrometer and a 256-channel spectrometer were used. Both of their detectors are single crystals. The spectrometer consists of a detector and an analyzer.

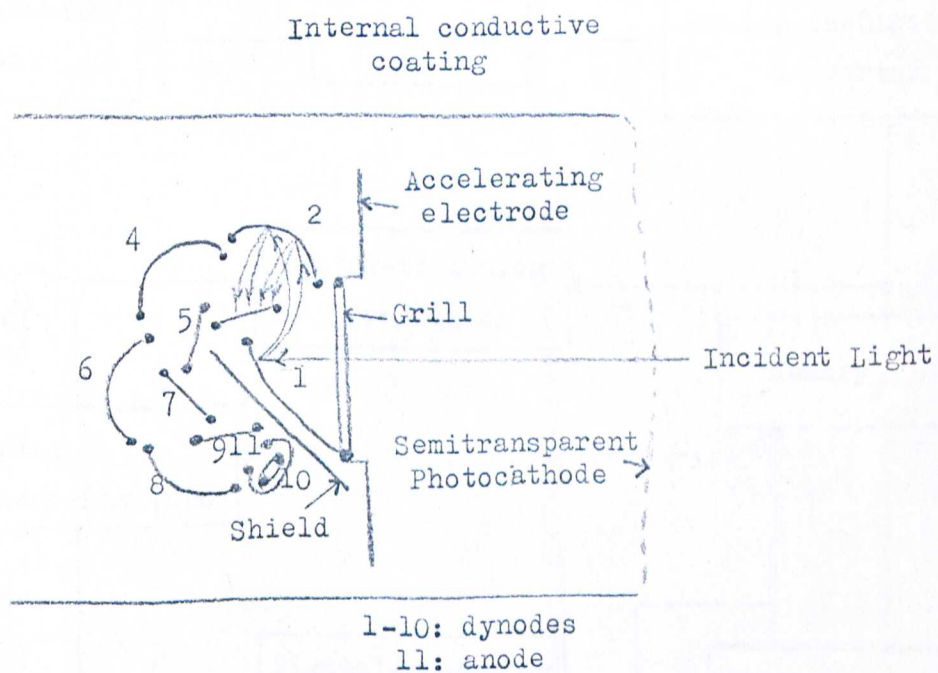
a. Detector. The detector consists of a scintillation crystal, a light pipe and a photoelectron multiplier tube which is connected to the preamplifier of the analyzer as shown in Fig. 2-5 [5,9]. In the scintillation detector, flashes of light are emitted by NaI phosphor upon absorbing gamma rays.

The gamma ray being detected produces flashes of light in the scintillation crystal. By means of the light pipe and the reflector around the crystal, a large fraction of the light is transmitted to the photoelectron multiplier tube which consists of a photo-cathode followed by several stages of dynodes made of material possessing high secondary electron emission properties. The photo-cathode converts a fraction of the radiation falling on it into photoelectrons which are multiplied many times by means of the dynodes. The resulting current pulse then produces a voltage pulse at the input of the preamplifier of the analyzer.

b. Analyzer [10] Single-channel pulse height analyzer contains the elements shown in Fig. 2-6. The differential discrimination of the single channel consists of two discriminator circuits with a small, adjustable difference in their triggering thresholds so that signals in small voltage range ΔV , often referred to as window width,



Schematic Diagram of a Scintillation Detector



Schematic Diagram of a Photomultiplier [9]

Fig. 2.5

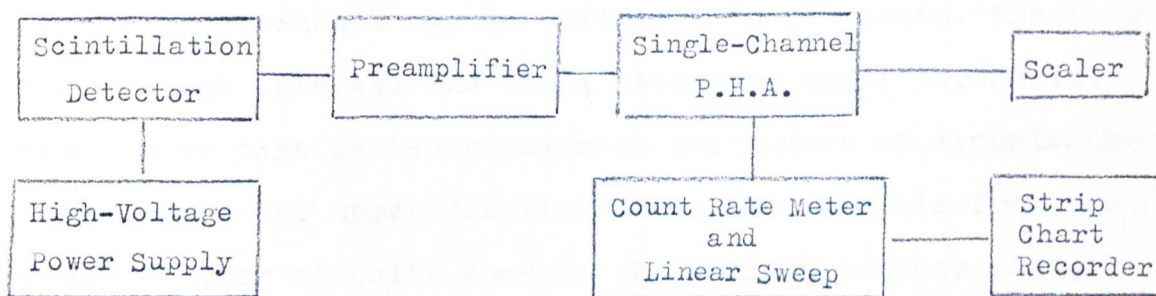


Fig. 2.6 [11]

Schematic Diagram of a Single-Channel Analyzer

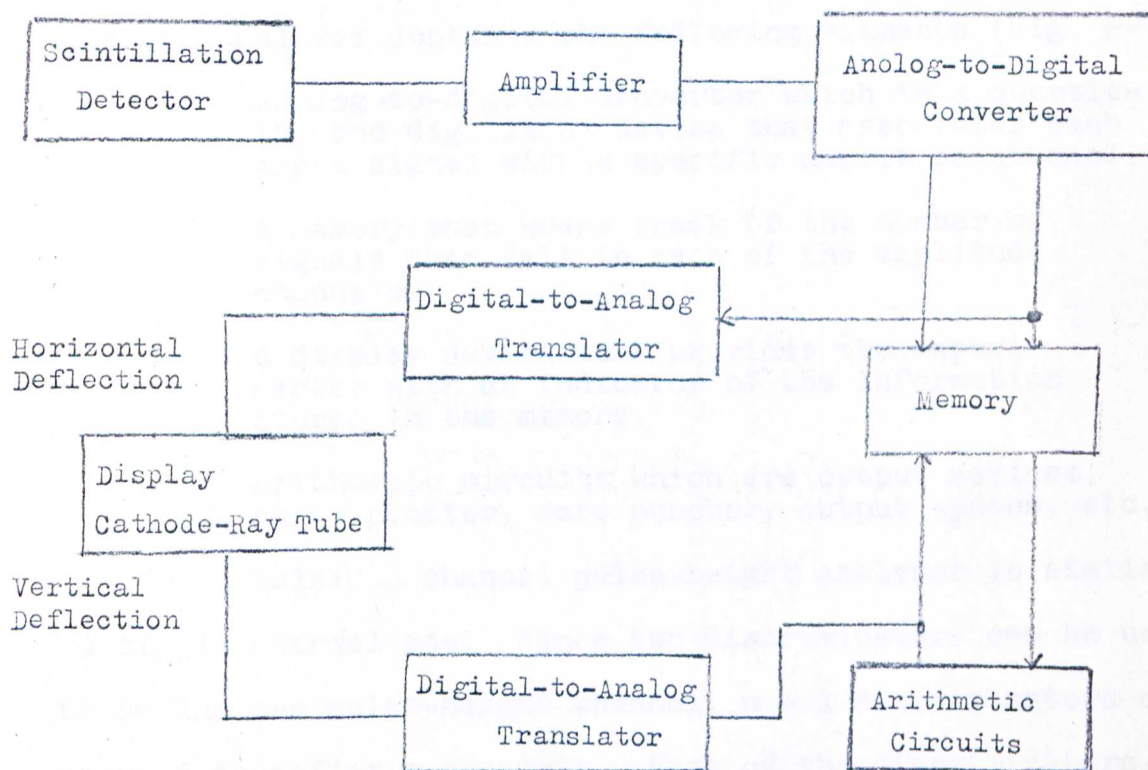


Fig. 2.7 [12]

Schematic Diagram of a Multiple-Channel Analyzer

exceeds one threshold but not the other. Signals exceeding the lower threshold can be divided into two parts, those in the voltage interval and those above the upper threshold. The latter part is identical with the number of signals obtained from the upper discriminator. The signals from the discriminator circuits come to the anticoincidence circuit cancels all signals above the upper threshold so that only signals that fall in the voltage range ΔV are passed on to the scaler or the count rate meter and linear sweep. In the single channel analyzer there is an automatic interlocking switch for removal of the high bias voltage prior to opening.

Multi-channel pulse height analyzer. The 256-channel analyzer contains the following elements (Fig. 2-7)

Analog-to-digital converter which is a quantizing and digitizing device that associates each input signal with a specific amplitude channel.

A memory that keeps track of the number of signals that fall in each of the amplitude channels.

A display device that provides the experimenter with an indicator of the information stored in the memory.

Arithmetic circuits which are output devices, curve plotter, card puncher, output system, etc.

Multi-channel pulse-height analyzer is similar to single channel one. Since two discriminators can be used to define one pulse-height channel, $n + 1$ discriminators can be used to define n channels. Each of the discriminators, except the first and the last, defines the upper edge of one channel and the lower edge of the next channel.

2-3 G.M. Survey meter

A Nuclear Chicago Model 2616 Geiger Müller (G.M.) counter was used in the gamma ray shielding survey. As stated previously, it has 3 ranges of 0-0.2 mr/hr, 0-2 mr/hr and 0-20 mr/hr. The G.M. tube is contained in a probe attached to the portable instrument box by means of a cable. The high voltage required to operate the tube is supplied by batteries contained in the box. The pulses from the tube, caused by incident radiation, are amplified and fed to a count-rate meter calibrated in mr/hr and to a pair of headphones.

This G.M. survey meter detects both gamma rays and beta particles when the window of the tube is open and it detects gamma rays only when the window is covered with a metal shield. The principle of the G.M. survey meter is based on the ionization chamber which is operated at a voltage in the G.M. region. In that region, all pulses have the same size no matter what the initial ionization is.

2-4 Calibration Sources

A small Co^{60} source which emits gamma rays of 1.33 Mev and 1.17 Mev, and a small Cs^{137} source with one gamma ray of 0.662 Mev from New England Nuclear Corp. were used to calibrate the spectrometer. Another Co^{60} source with a strength of 4.7 millicuries on December 8, 1960, with half life 5.3 years was used to calibrate the G.M. survey meter.

III PROCEDURE AND EXPERIMENTAL DATA

3-1 Procedure

These studies consist of two parts: the measurement of gamma ray spectra and the shielding survey of the reactor. The former was measured at three positions: the west beam tube, the thermal column and the top of the reactor. The latter consisted of the measurement of the dose rates on the wall and the concrete top of the reactor.

At the beam tube, one or two shielding plugs were removed for measurements. The gamma ray beam was collimated by a lead-concrete-paraffin collimator to the spectrometer detector which was shielded by lead bricks.

At the thermal column, the small plug and the lead block were taken out. As in the beam tube arrangement, the gamma ray beam through the thermal column was collimated to the spectrometer detector. However, because of the thermal column geometry, the collimator was formed by paraffin and the detector was shielded by paraffin.

In contrast with the geometries at the above positions, no collimator was used at the top of the reactor. The spectrometer detector was held above the water surface of the pool by means of a wooden support.

For the shielding survey, the surface areas of the wall and the concrete top of the reactor were divided into squares of 1' x 1'. The dose rate, when the reactor was

at full power, was measured at the center of the square by means of the G. M. survey meter which was calibrated with the Co^{60} source.

3-2 Single Channel Spectrometer Gamma Ray Spectra

Most of the gamma ray spectra in the experiment were recorded by the single channel spectrometer at three positions. The west beam tube, the thermal column and the top of the reactor. This spectrometer takes thirty minutes for each full spectrum, i.e. the spectrum is obtained when the automatic discriminator switch is moving from 1000 volts to zero.

a. The spectra recorded at the west beam tube were divided into two sets; the gamma ray spectra when the reactor was shut down and the gamma ray spectra when the reactor was operating.

Fig. 3-1 shows the spectrum of the first set which was measured under the following conditions:

- (1) two plugs were taken out,
 - (2) the detector was at 30 cm from the wall of the reactor,
 - (3) the cross section of the collimator was about 1.5 cm x 1.5 cm,
- and
- (4) the reactor had been shut down for about 15 hours after being operated at full power for about 3 hours.

Since the intensity of the gamma ray beam from the core through the beam tube was too high when two plugs were out, the spectrum was out of scale below 2 Mev even when the

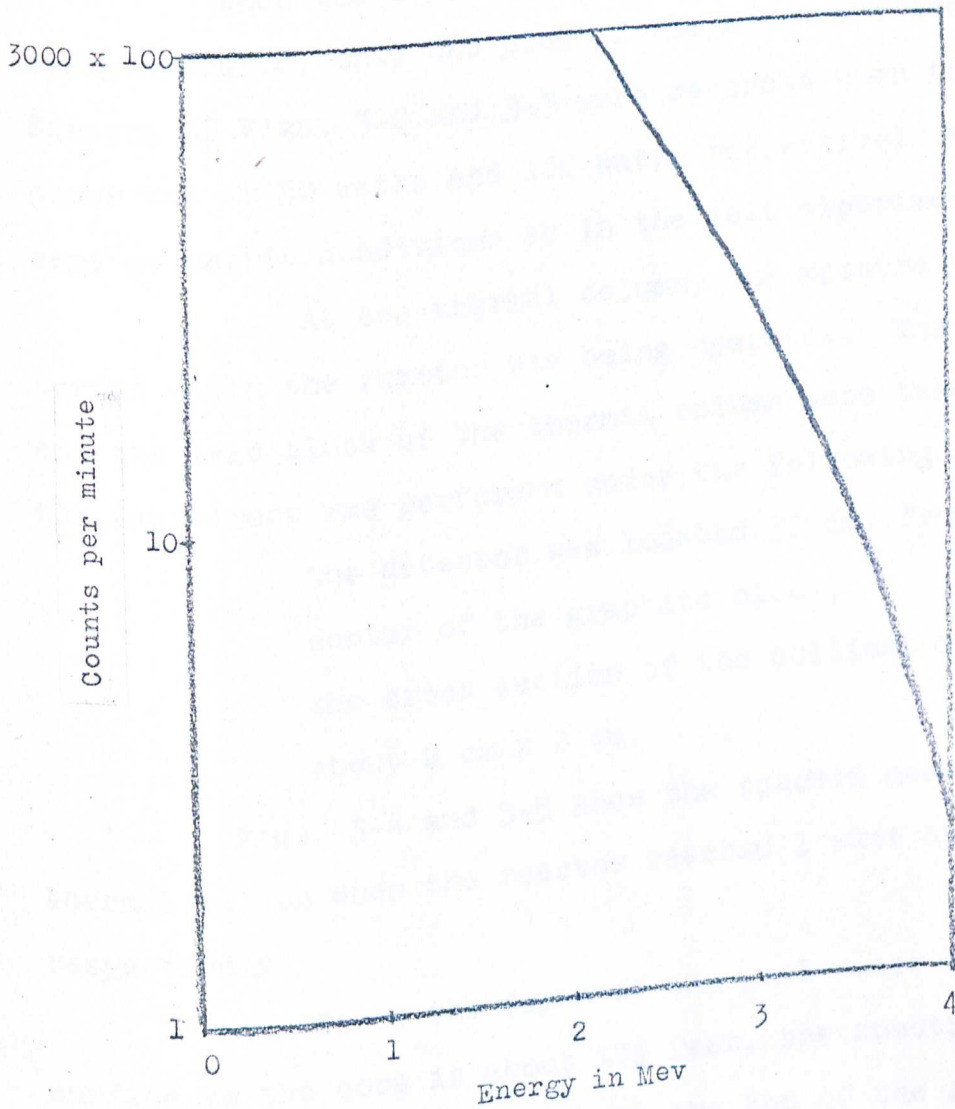


Fig. 3.1

Gamma Spectrum I
 Position: Beam Tube, two Plugs out
 Time after Shutdown: 15 Hours
 Spectrometer: Single-Channel, Window 2

uppermost range of 300 k, i.e. 300,000 counts per minute was used.

When the experiment was performed with the reactor being operated, only one plug of the beam tube was taken out. Spectra of Figs. 3-2 and 3-3 were recorded when the reactor power was at 50 watts and 100 watts respectively with the same geometric conditions as in the last experiment.

b. At the thermal column, the spectra were recorded while the reactor was being operated. The small plug and the lead block of the thermal column were taken out and the experiment was performed under the following conditions: the detector was located 30 cm. from the center of the graphite block, the cross section of the collimator was about 2 cm x 2 cm.

Figs. 3-4 and 3-5 show the spectra measured at the thermal column when the reactor reached 1 watt and 5 watts respectively.

c. Since the depth of the pool water from the pool surface to the core is about $17\frac{1}{2}$ feet, the spectrum was recorded at full power of 10 kw at the top of the reactor.

The spectrum (Fig. 3-6) was recorded when the reactor was at full power for about 3 hours and the detector was placed at the center of the pool and at 2.5 cm above the surface of pool water.

3-3 Multi-Channel Spectrometer Gamma Ray Spectra

Although the single channel pulse height spectrometer is adequate for measurements of reactor core gamma ray

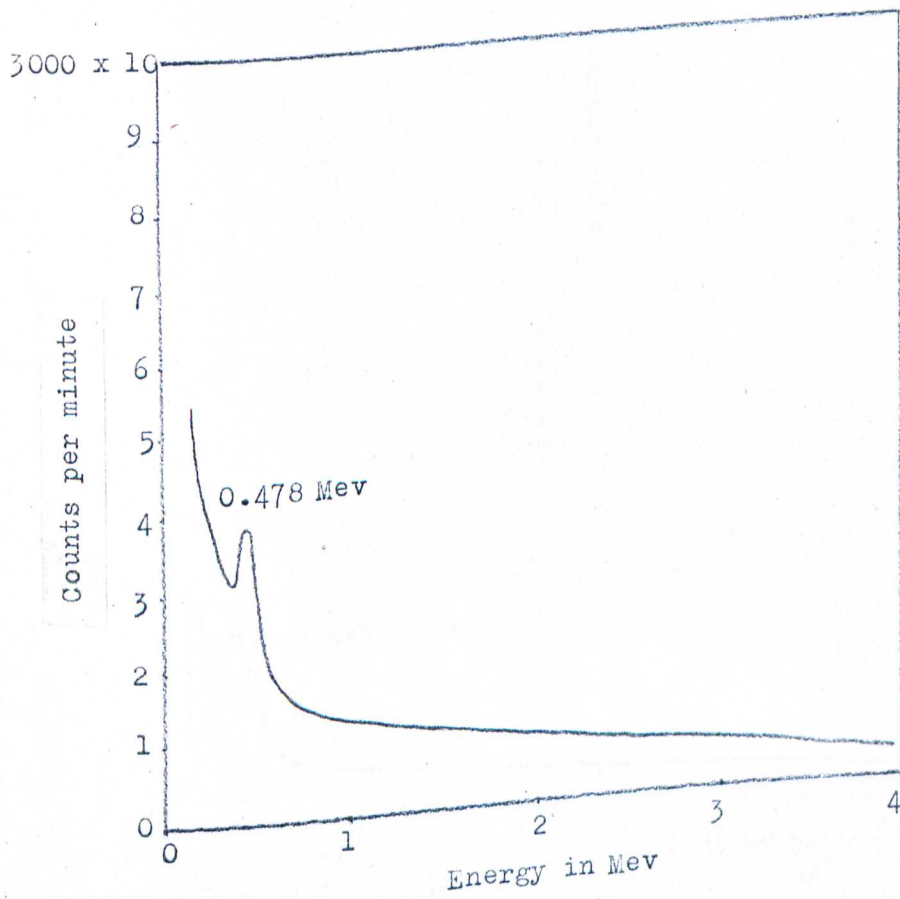


Fig. 3.2

Gamma Spectrum II

Position: Beam Tube, one Plug out

Power: 50 Watts

Spectrometer: Single-Channel, Window 2

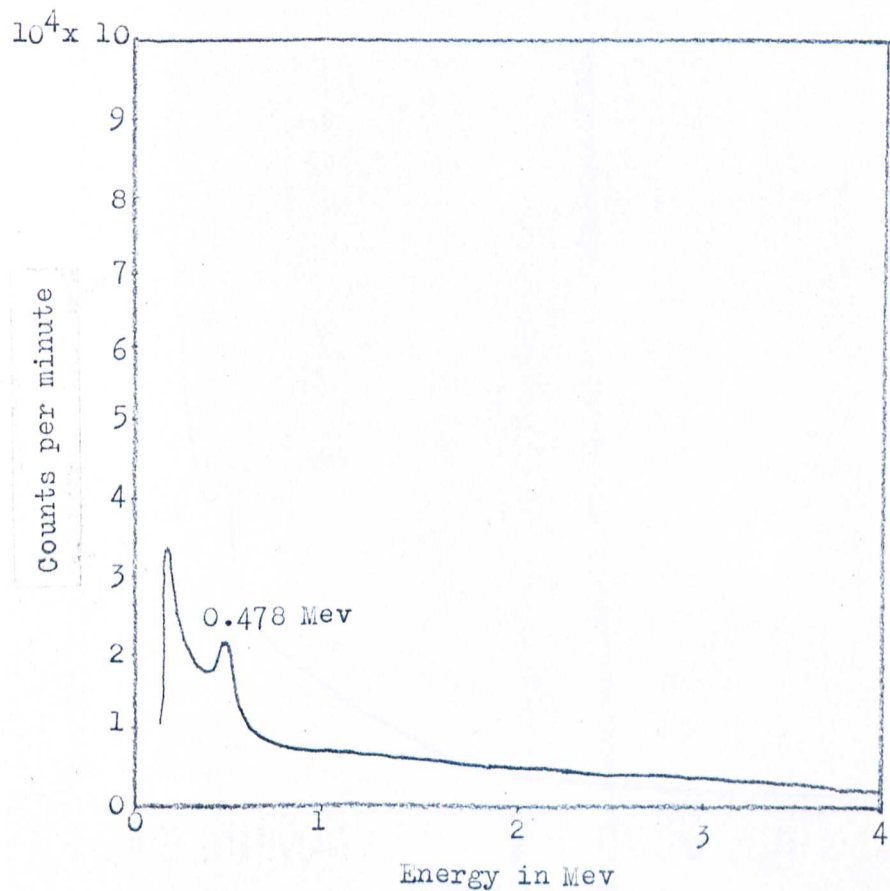


Fig. 3.3

Gamma Spectrum III

Position: Beam Tube, one Plug out

Power: 100 Watts

Spectrometer: Single-Channel, Window 2

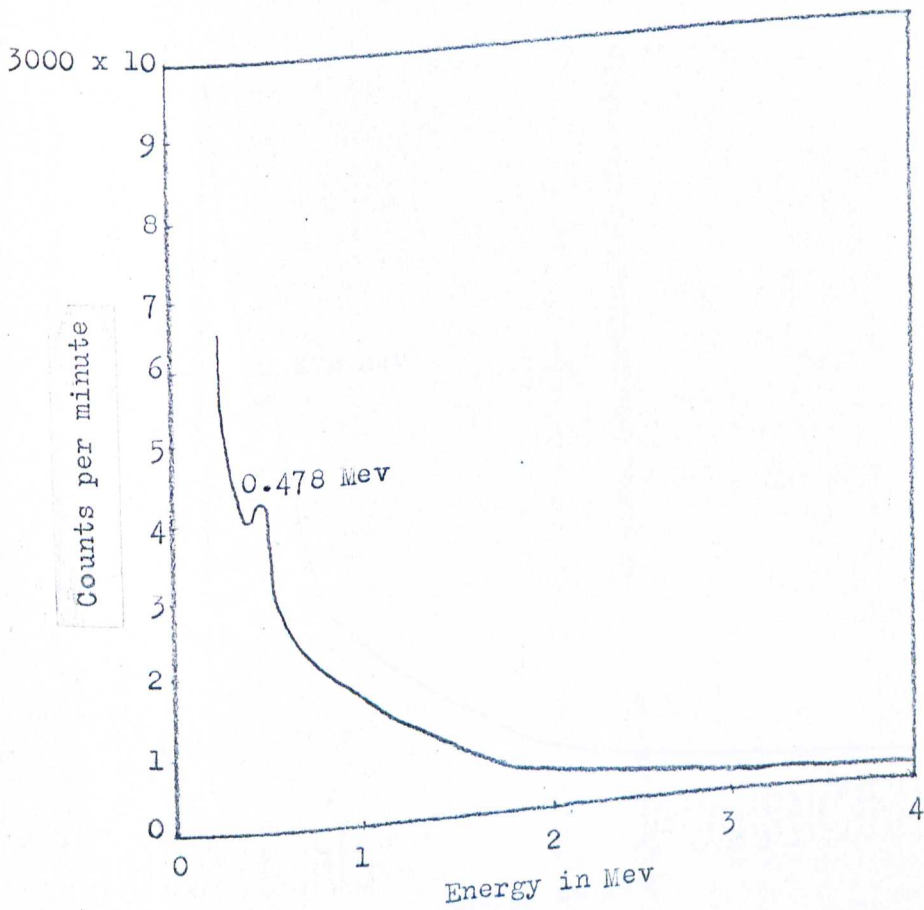


Fig. 3.4
 Gamma Spectrum IV
 Position: Thermal Column, Small Plug out
 Power: 1 Watt
 Spectrometer: Single-Channel, Window 1

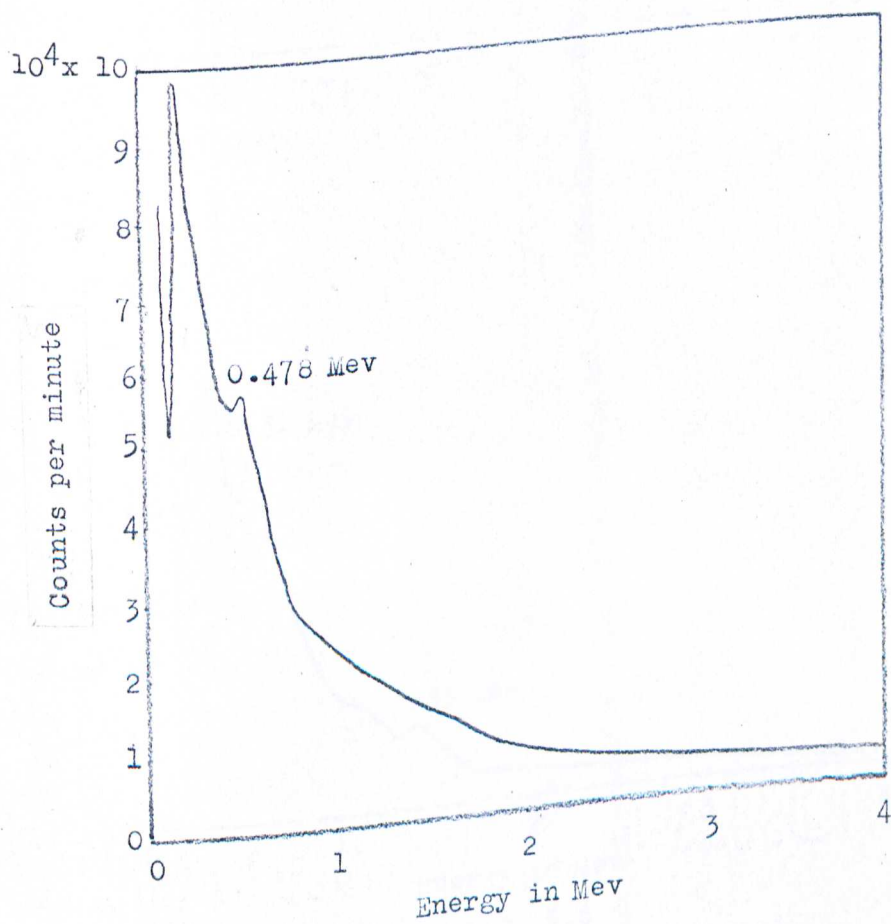


Fig. 3.5
Gamma Spectrum V
Position: Thermal Column, Small Plug out
Power: 5 Watts
Spectrometer: Single-Channel, Window 1

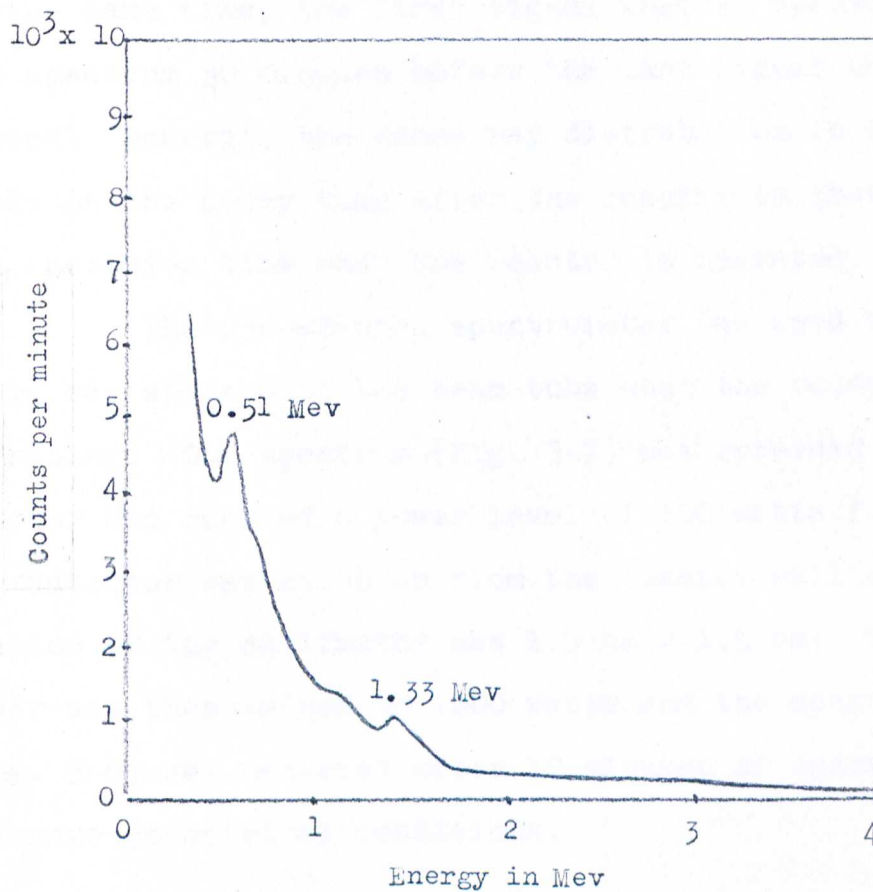


Fig. 3.6

Gamma Spectrum VI

Position: Top of the Reactor

Power: 10 Kilowatts

Spectrometer: Single-Channel, Window 1

spectra, it has some disadvantages for certain experiments. In the single channel spectrometer, the signals that are fed into the spectrum recorded do not come to the single channel at the same time, the first signal that is recorded, comes to the spectrum 30 minutes before the last signal that is recorded. However, the gamma ray distribution in the core depends on the decay time after the reactor is shut down and on the operation time when the reactor is operated.

The 256-channel spectrometer was used to record gamma ray spectra at the beam tube when the reactor was operating. One spectrum (Fig. 3-7) was recorded after the reactor had reached a power level of 100 watts for 15 minutes. The detector was at 40 cm from the reactor wall and the cross section of the collimator was 1.5 cm x 1.5 cm. The reactor power was then raised to 1000 watts and the second spectrum (Fig. 3-8) was measured after 10 minutes of operation under the same geometrical conditions.

3-4 Shielding Survey

The shielding survey was done on the wall and the concrete top of the reactor; the wall of the reactor is divided into 3 levels.

Figs. 3-9 — 3-14 show results of the shielding survey at the first level (0 - 11 ft.), while Figs. 3-15 and 3-16 are those at the second (11 - 13 ft.) and third (13 - 21 ft.) levels, respectively. The last one (Fig. 3-17) shows results of the survey at the top. Except for the last survey where the dose rates were measured with the scale at the range

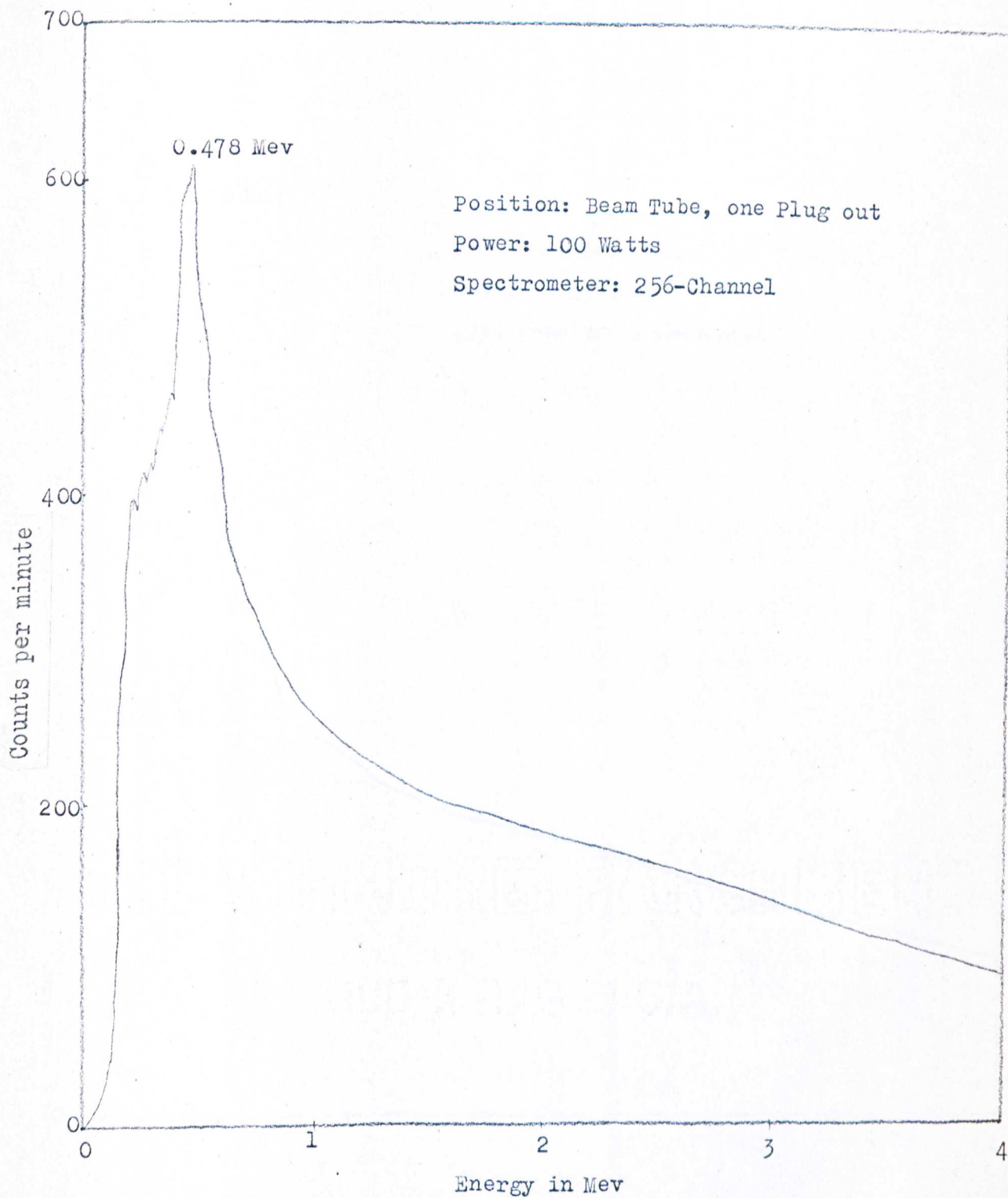


Fig. 3.7
Gamma Spectrum VII

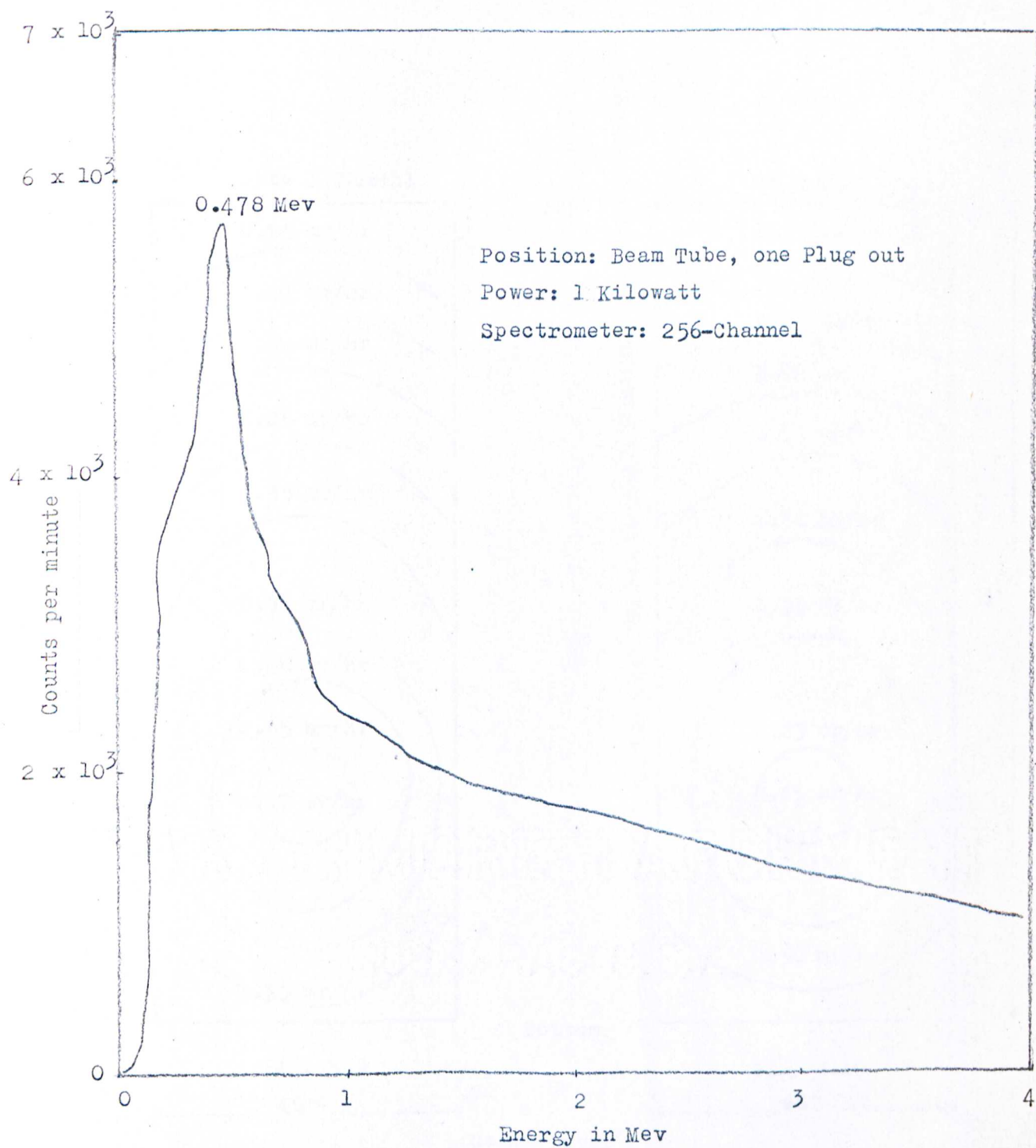


Fig. 3.8

Gamma Spectrum VIII

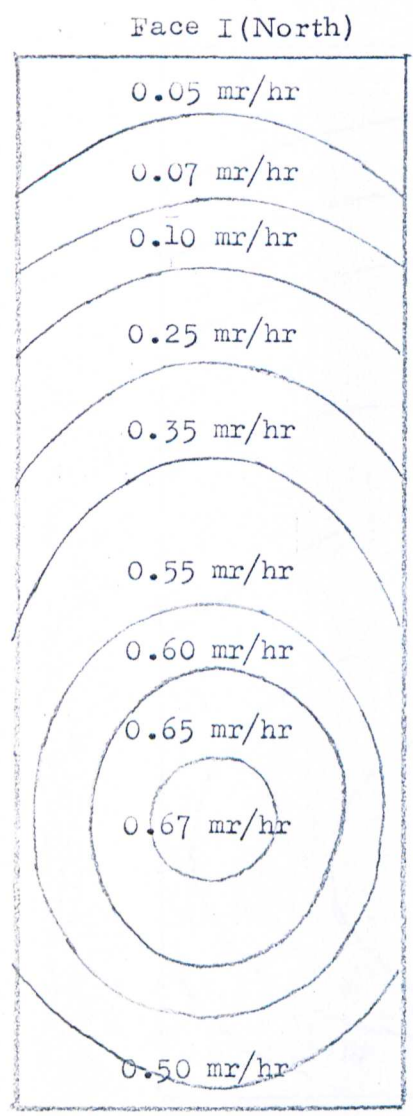


Fig. 3.9

48"

Top

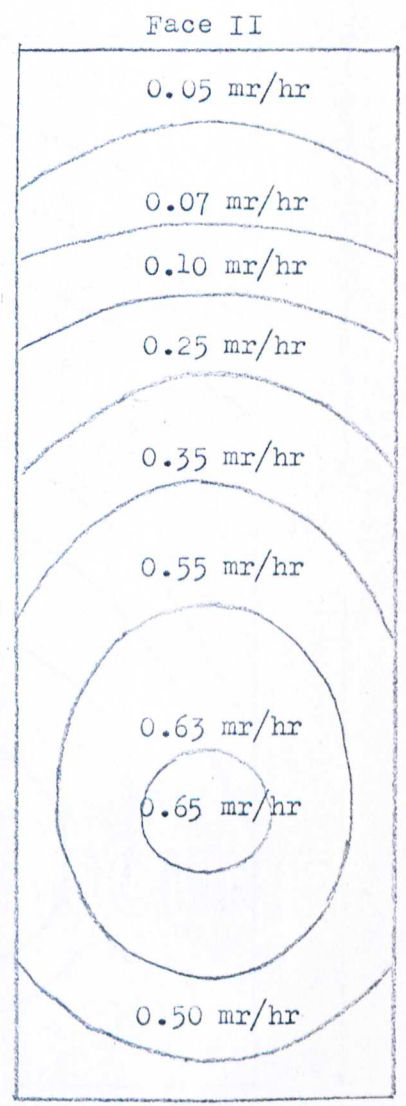


Fig. 3.10

48"

11'

Bottom

Gamma Level I

1 foot



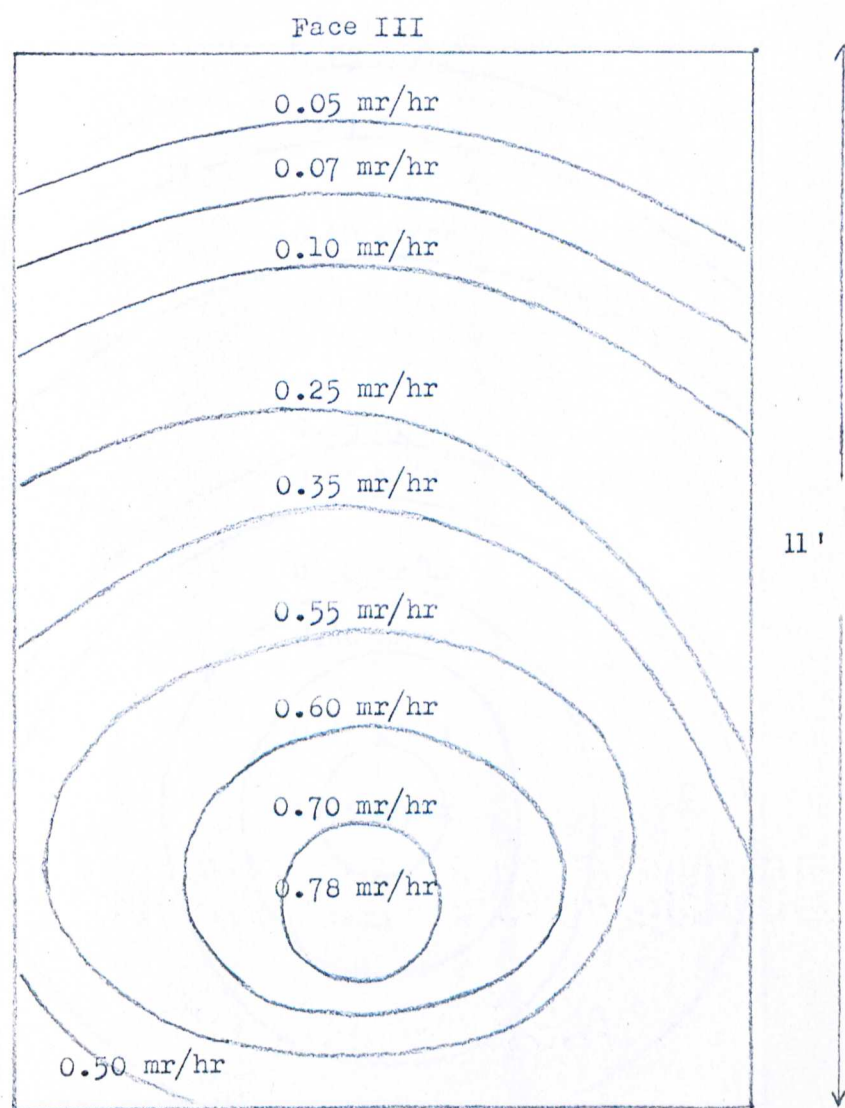


Fig. 3.11
Gamma Level I

1 foot



72"

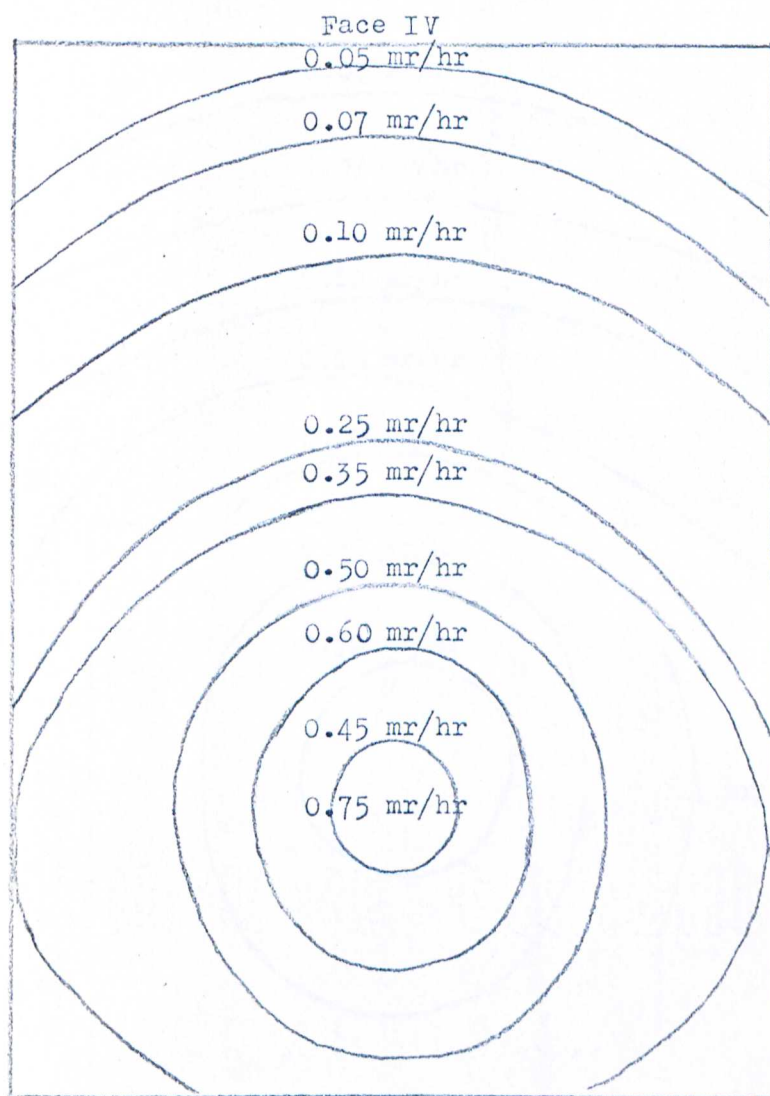


Fig. 3.12

Gamma Level I

1 foot



96"

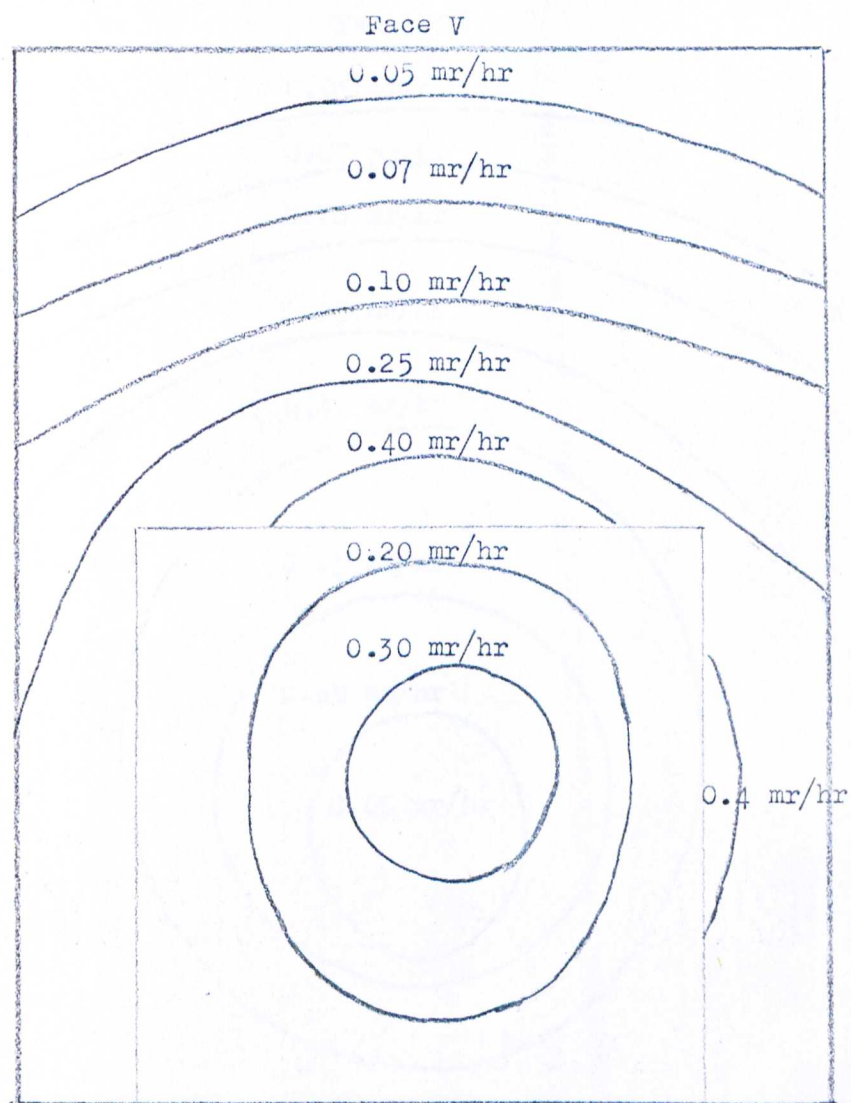
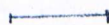


Fig. 3.13
Gamma Level I

1 foot



100"



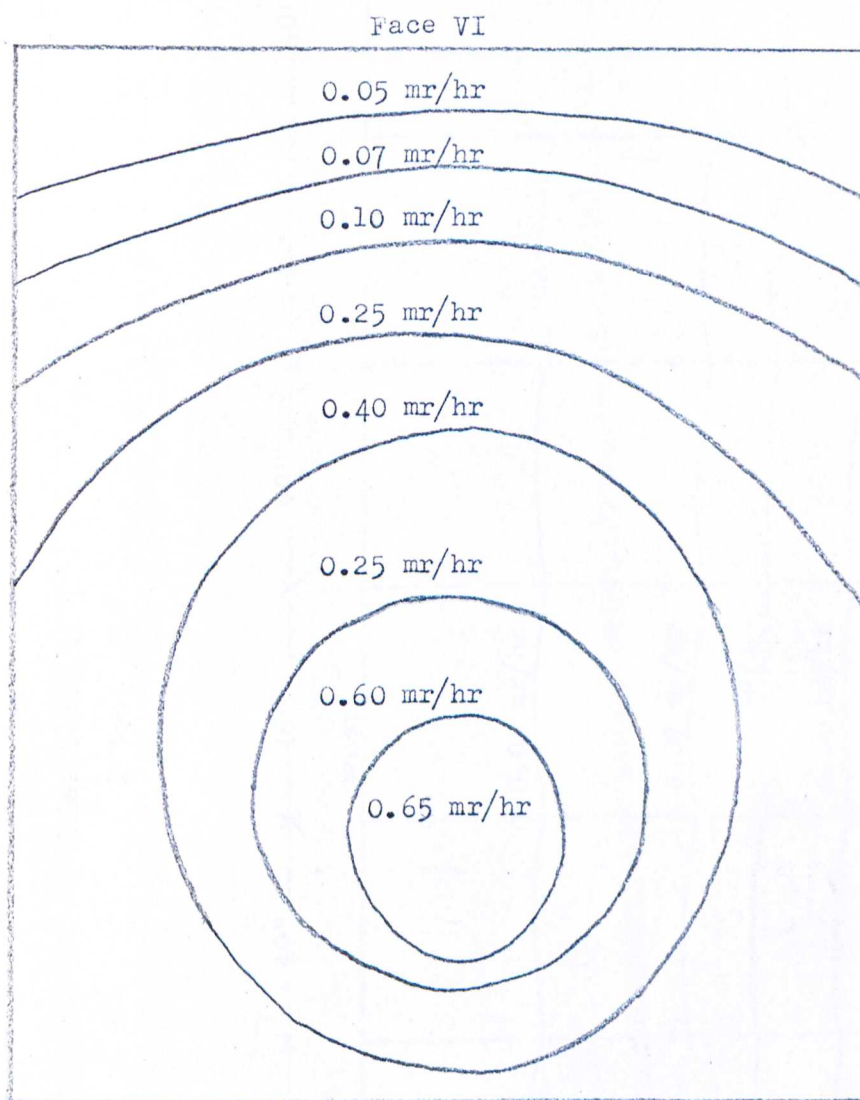


Fig. 3.14
Gamma Level I

1 foot



← 110" →

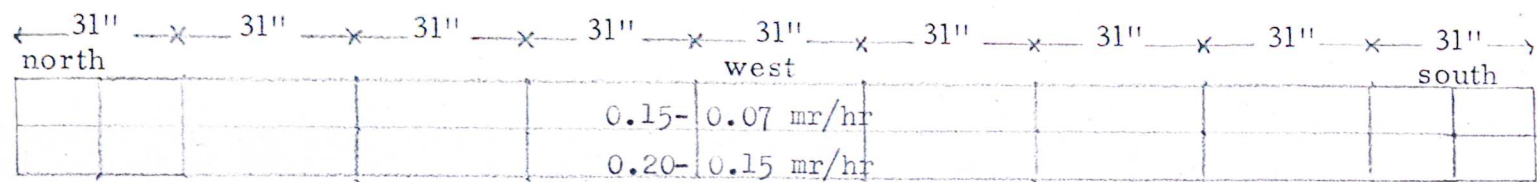


Fig. 3.15

Gamma Level II

1 foot

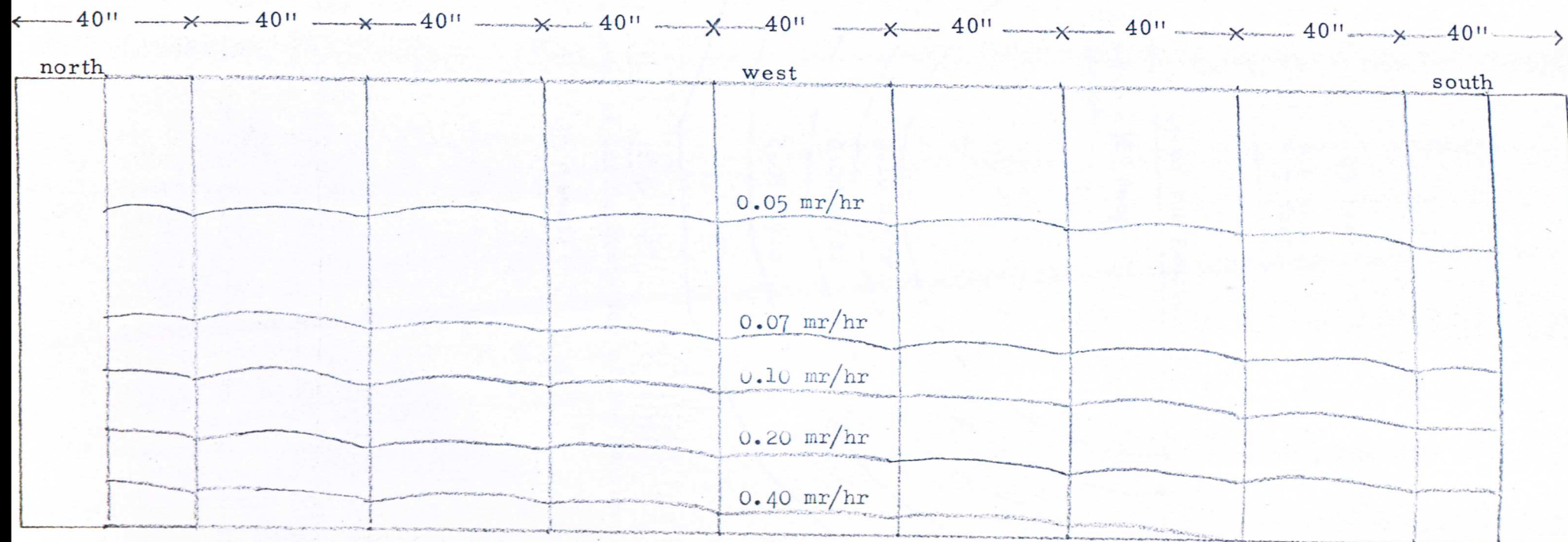


Fig. 3.16

Gamma Level III

1 foot



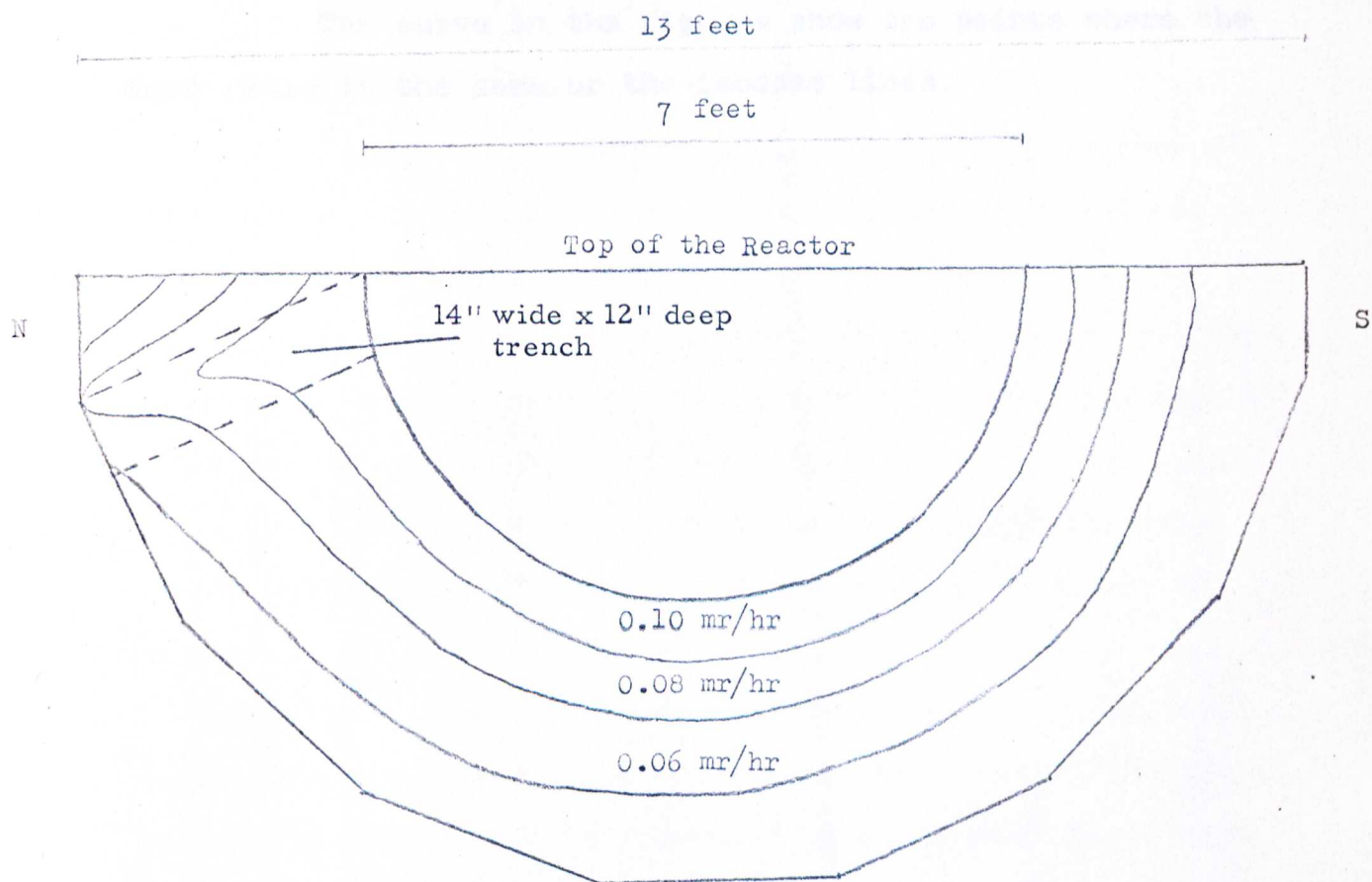


Fig. 3.17

Gamma Level at the Concrete Top of the Reactor

West

of 0-0.2 mr/hr, the dose rates at the other positions were measured with the scale at the range of 0-2 mr/hr.

The curve in the figures show the points where the dose ratio is the same or the isodose lines.

When the reactor is shut down the fission product gamma rays predominate. Since the spectrum (Fig. 3-1) was measured after a short period of decay, many short-lived isotopes were present. Furthermore, some of the short-lived decay are very energetic. It is very difficult to determine exactly what gamma rays were emitted [13].

However, the spectrum showed that the count rate or the intensity is approximately exponential function of energy.

Counts per minute (c/pm) = $Ce^{-1.18E}$

Under the same geometrical conditions, the constant C depends on the operation time before the reactor is shut down and on the decay time.

When the reactor is operated, the total amount of energy emitted is mostly from prompt fission gamma rays. Fission product gamma rays and neutron capture gamma rays. Although the amount of energy from these three sources, i.e. prompt fission, fission product and neutron capture gamma rays are comparable in magnitude, the neutron capture gamma rays tend to be more penetrating than the other two kinds [13].

All the spectra recorded at the beam tube and the thermal column consistently show a peak at 0.475 Mev, when the reactor was operated at different power levels. Since the

IV DISCUSSION

4-1 Gamma Ray Spectra

When the reactor is shut down the fission product gamma rays predominate. Since the spectrum (Fig. 3-1) was measured after a short period of decay, many short-lived isotopes were present. Furthermore, some of the short-lived decays are very energetic. It is very difficult to determine exactly what gamma rays were emitted [13].

However, the spectrum showed that the count rate or the intensity is approximately exponential function of energy

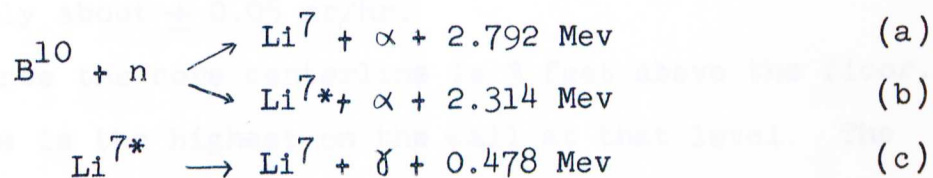
$$\text{Counts per minute (c/m)} = Ce^{-1.18E}$$

Under the same geometrical conditions, the constant C depends on the operation time before the reactor is shut down and on the decay time.

When the reactor is operated, the total amount of energy emitted is mostly from prompt-fission gamma rays, fission-product gamma rays and neutron capture gamma rays. Although the amount of energy from these three sources, i.e. prompt fission, fission product and neutron capture gamma rays are comparable in magnitude, the neutron capture gamma rays tend to be more penetrating than the other two kinds [13].

All the spectra recorded at the beam tube and the thermal column consistently show a peak at 0.478 Mev, when the reactor was operated at different power levels. Since the

radiation from the core through the centerlines of the beam tube and the thermal column must penetrate $1/8$ in. boron in these experiments, it is quite probable that the peak is due to boron -10. Boron-10 has very high thermal neutron cross section 3390 barns and it gives rise to a 0.478 Mev gamma ray as a result of neutron capture:



For thermal neutron, 94 per cent of the disintegrations pass through reaction (a) [14]. In some spectra (Figs. 3-3 and 3-5) there are peaks due to characteristic X-rays. However the resolution of the spectrometer is not sufficiently accurate to identify these characteristic X-rays. The gamma ray intensity was found to be proportional to the reactor power.

The spectrum at the reactor top shows a clear peak at 0.51 Mev which is due to annihilation radiation. The other peak is at 1.33 Mev. It is possible that this peak is due to I^{136} , since the yield of I^{136} from fission of U^{235} is high [15]. Usually, the lower portion of the different spectra taken with the reactor running can be considered as being approximately a linear function of energy.

Reactor core gamma ray spectra are supposed to have a peak at 2.23 Mev which is due to the thermal neutron capture gamma ray of hydrogen; however the shield around the core is thick and the thermal neutron cross-section of hydrogen is not large, 0.33 barn. Furthermore, the spectrum of core gamma

rays is really a superimposition of many spectra; these probably account for the fact that the peak of that gamma ray was not seen in the above spectra.

4-2 Shielding Survey

The dose rates shown in Figs. 3-9 — 3-17 are accurate to only about ± 0.05 mr/hr.

Since the core centerline is 3 feet above the floor, the dose rate is the highest on the wall at that level. The reactor core is not exactly in the center of the pool but it is closer to the south side than to the north side. However, the dose rate from the core streaming through the thermal column was reduced by 4 inches of lead placed inside the thermal column in front of the concrete plug and the dose at the adjacent faces was reduced by the addition of steel plates on the outer wall of the adjacent faces. Therefore the dose rates at the thermal column face and the adjacent faces were lower than those at the other faces.

The maximum dose rate at the 3 feet above the floor and on the wall of the reactor is about 0.8 mr/hr. This value is approximately equal to the calculated value using the point source model and the build-up factor of $1 + 2\mu x$ (Appendix). Because of the effect of multi-scattering in the shield, the build-up factor of $1 + \mu x$ gives a calculated value lower than the measured value.

V CONCLUSIONS AND RECOMMENDATIONS

The gamma ray spectra of the University of Maryland reactor core measured at different power levels are linear in the part of 1-2 to 4 Mev which is the second important range of energy in the shielding problem.

Since high energy gamma rays are the most important in shielding, it is recommended that gamma ray spectra of the University of Maryland reactor be measured by a multiple-channel spectrometer with a wider range of energy, if the intensity from the core is very high, perhaps a dead time correction should be made. Measurement of the gamma ray spectra of the operating core requires a low neutron induced background and high resolution, a multiple-crystal spectrometer might be useful here.

The effect of multiscattering of the gamma rays from the core requires using $1 + a\mu x$ as the build-up factor for the point source model instead of the build-up factor of $1 + \mu x$ where a is constant and $\mu x = \sum_i \mu_i x_i$ for laminated shield (Appendix); the constant a depends on the thickness and materials of the shield. In the case of the University of Maryland reactor, a is equal to 2.

In the calculation of the reactor dose rate, the choice of average gamma ray energy is approximate. It is recommended that (a) the neutron capture gamma ray energy be calculated from the constitution of the core, (b) the

gamma ray spectrum be divided into a number of discrete energy groups e.g. at 1, 2..., 8 Mev and finally, (c) the dose rate be obtained by adding these contributions.

Calculated Value of the Dose Rate at the Outside Wall of the University of Maryland Reactor at Core Level

With the point source model, the gamma ray flux Φ at the distance R in cm from the point source is given by

$$\Phi = I_0 B \frac{e^{-\mu x}}{4\pi R^2} \quad \text{Neutrons/cm}^2 \quad (1)$$

where I_0 is the intensity in Mev/sec of the point source; it is proportional to the power level of the reactor

B is the build-up factor

μ is the gamma ray attenuation coefficient of 1 in material, in cm^{-1}

x is the thickness of 1 th material.

On the basis of 190 ± 5 Mev of useful energy emitted per fission [17], about 3.3×10^{13} fissions per second yield 1 Mw of thermal power. Thus, the number of fissions per second in the core is

$$3.3 \times 10^{13} P \text{ fissions/sec.} \quad (2)$$

where P is the power level, in Mw.

As stated in the Introduction, there are three principal gamma ray sources in the reactor core: (1) about 7.5 Mev of prompt gamma rays per fission, (2) gamma decay of fission products in equilibrium operation gives 9 Mev per fission, (3) in a reactor using ^{235}U , 1.9 neutrons produced per fission are captured in nonfissionable material, releasing

APPENDIX

Calculated Value of the Dose Rate at the Outside Wall of the University of Maryland Reactor at Core Level

With the point source model, the gamma ray flux J at the distance R in cm from the point source is given by

$$J = I_0 B \frac{e^{-\sum \mu_i x_i}}{4 R^2} \text{ Mev/sec/cm}^2 \quad (1)$$

where I_0 is the intensity in Mev/sec of the point source; it is proportional to the power level of the reactor

B is the build-up factor

μ_i is the gamma ray attenuation coefficient of i th material, in cm^{-1}

x_i is the thickness of i th material.

On the basis of 190 ± 5 Mev of useful energy emitted per fission [18], about 3.3×10^{13} fissions per second yield 1 Kw of thermal power. Thus, the number of fissions per second in the core is

$$S = 3.3 \times 10^{13} P \text{ fissions/sec.} \quad (2)$$

where P is the power level, in Kw.

As stated in the Introduction, there are three principal gamma ray sources in the reactor core: (1) about 7.5 Mev of prompt gamma rays per fission, (2) gamma decay of fission products in equilibrium operation gives 5 Mev per fission, (3) in a reactor using U^{235} , 1.5 neutrons produced per fission are captured in nonfissionable material, releasing

about 7 Mev per capture [9]. Then, there are a total of about 23 Mev of gamma rays per fission. The point source intensity I_0 is given by

$$I_0 = 3.3 \times 10^{13} \times 23 P \text{ Mev/sec} \quad (3)$$

Although each gamma ray has a specific energy, practically, there is a continuous distribution; approximately the energy distribution may be considered to have an average energy 3 Mev [9]. The ratio of gamma flux to dose rate J/D depends on the energy, however, from 60 Kev to about 7 Mev that ratio differs by no more than 25% from the value appropriate for 2.5 Mev [16]

$$\frac{J}{D} = 6.50 \times 10^5 \text{ Mev/cm}^2 \cdot \text{sec per r/hr} \quad (4)$$

where D is given in roentgens per hour. From Eqs. (1), (3) and (4)

$$D = \frac{3.3 \times 10^{13} \times 23}{6.5 \times 10^5} \text{ PB } \frac{e^{-\sum \mu_i x_i}}{4 R^2} \text{ r/hr} \quad (5)$$

or

$$D = 1.17 \times 10^{12} \text{ PB } \frac{e^{-\sum \mu_i x_i}}{4 R^2} \text{ r/hr} \quad (6)$$

The build-up factor B can be given by [16]

$$B = 1 + a(\mu x)^k \quad (7)$$

where a and k are constant

μ is the attenuation coefficient for shield

x is given by [9]

$$x = \frac{\sum \mu_i x_i}{\mu} \quad \text{for laminated shield.}$$

In the case of the University of Maryland reactor, two main materials are present:

water μ_w at 3 Mev = 0.0398 cm^{-1} [17]

thickness of water $x_1 = 3\frac{1}{2}' = 106.68 \text{ cm}$

concrete μ_2 at 3 Mev = 0.073 cm⁻¹

thickness of concrete $x_2 = 7' = 213.35$ cm

then

$$\mu x = \mu_1 x_1 + \mu_2 x_2 = 4.25 + 15.6$$

$$\mu x = 19.85$$

Hence

$$D = 1.17 \times 10^{12} \times \frac{1.4264}{10^2} \times \frac{1.68}{10^7} \times \frac{1}{4 \pi \times 1.025 \times 10^5}$$

$$\times \left[1 + a(19.85)^k \right] P \text{ mr/hr}$$

or

$$D = 2.17 \times 10^3 \left[1 + a(19.85)^k \right] P \text{ mr/hr}$$

with the power level of 10 kw and assuming $k = 1$ [16]

$$D = 2.17 \times 10^2 \left[1 + 19.85 a \right] \text{ mr/hr}$$

If $a = 1$ $D = 0.453$ mr/hr

If $a = 2$ $D = 0.862$ mr/hr

SELECTED BIBLIOGRAPHY

1. Etherington, H., "Nuclear Engineering Hand Book", McGraw-Hill Book Company Inc., New York, 1958.
2. Rockwell III, T., "Reactor Shielding Design Manuel", McGraw-Hill Book Company, Inc., New York, 1956.
3. Mittelman, P. S. and Liedtke, R. A., "Nucleonics", May, 1955.
4. Glasstone, S., "Principles of Nuclear Reactor Engineering", D. Van Nostrand Company, Inc., New Jersey
5. Evans, R. P., "The Atomic Nucleus", McGraw-Hill Book Company, Inc., New York, 1955.
6. Price, W. J., "Nuclear Radiation Detector", McGraw-Hill Book Company, Inc., New York, 1958.
7. Ajzenbergl-Selove, "Nuclear Spectrometry - Part B", Academic Press, New York, 1960.
8. Nuclear Engineering Staff", Safeguards Evaluation of the University of Maryland Reactor", University of Maryland, 1960.
9. Bonilla, C. F., "Nuclear Engineering", McGraw-Hill Book Company, Inc., New York, 1957.
10. Chase, R. L., "Nuclear Pulse Spectrometry", McGraw-Hill Book Company, Inc., New York, 1961.
11. Crouthamel, C. E., "Applied Gamma Ray Spectrometry", Pergamon Press, New York, 1960.
12. Schumann, R. W., and McMahon, J. P., "Review of Scientific Instrucments", 27: September, 1956.
13. Price, B. T., Horton, C. C., and Spinney, K. T., "Radiation Shielding", Pergamon Press, New York, 1957.
14. Allen, W. D., "Neutron Detection", Philosophical Library, Inc., New York, 1960.
15. Katcoff, S., "Nucleonics", 16: April, 1958.

16. Goldstein, H., "Fundamental Aspects of Reactor Shielding", Addison-Wesley Publishing Company, Inc., Massachusetts, 1959.
17. Goldstein., and Wilkins, Jr., J. E., "NYO-3075", June 30, 1954.
18. Meem, J. L., "Nucleonics", 12: May, 1954.
19. Blizard, E. P., "Reactor Handbook - Volume III, Part B Shielding," Interscience Publishers, 1962.

Date of birth: May 21, 1937

Place of birth: Quang Ngai, VIET-NAM

Secondary education: Khai Dinh Lycee, Hue, VIET-NAM, 1955

Collegiate Institutions attended	Dates	Degree	Date of Degree
University of Saigon, VIET-NAM	1955-1959	Licence de Sciences Mathematiques	1959
University of Maryland, U.S.A.	1961-1963	M.S.	1963

Major: Nuclear Engineering

Minor: Mathematics